University of Nevada, Reno

Hydrometallurgical recovery of critical metals from NMC 523 powders and its associated environmental impacts

A thesis submitted in partial fulfillment of the requirements for

the degree of Master of Science in

Metallurgical Engineering

by

Hector Solorio Arteaga

Dr. Ehsan Vahidi/Thesis Advisor

December 2021

THE GRADUATE SCHOOL

We recommend that the thesis
prepared under our supervision
by

Hector Solorio

entitled

**Hydrometallurgical recovery of critical metals from
NMC523 powders and its associated environmental
impacts**

be accepted in partial fulfillment of
therequirements for the degree of

MASTER OF SCIENCE

Ehsan Vahidi, Ph.D.
Advisor

Carl Nesbitt, Ph.D.
Committee Member

Dev Chidambaram, Ph.D.
Graduate School Representative

David W. Zeh, Ph.D., Dean
Graduate School

December 2021

Abstract

The lithium-ion battery industry's accelerated growth is raising interest in the recycling of valuable metals. Lithium, manganese, cobalt, and nickel can be recovered from the cathode powders using inorganic acids like hydrochloric acid (HCl), nitric acid (HNO_3), and sulfuric acid (H_2SO_4) in the leaching process. The experiments were designed using a statistical tool to optimize the parameters involved in the leaching process such as temperature, leaching time, concentration of leaching agents, solid to liquid ratio, and %volume of H_2O_2 to yield the best results for lithium recovery (%), nickel recovery (%), cobalt recovery (%) and manganese recovery (%). This study provides optimized leaching parameters, a detailed environmental impact assessment to identify the best inorganic acid in each category as well as the component contribution for each inorganic acid in all the categories included in the life cycle assessment (LCA) study, and a comparison of co-additives using the optimal conditions of the best performing leaching agent. The optimal conditions for each acid were H_2SO_4: 1.97 M, 69.99ºC, 20 min, L/S:0.091, and 0.957 H_2O_2 conc. (v/v%), HCl: 1.611 M, 69.99ºC, 89.9 min, L/S:0.098, and 0.99 %H_2O_2 conc (v/v%), and HNO_3: 0.62 M, 58.2ºC, 58.7 min, L/S:0.097 and 0.66 H_2O_2 conc. (v/v%). After analyzing the environmental performance for each acid, it was found that depending on the impact category, each acid has more emissions than the others. Overall, H_2SO_4 showed the best environmental and operational performance among all inorganic acids to recover critical materials from NMC 523 cathode powders.

To my family, friends, and everyone

who supported me through this journey,

Acknowledgements

I would like to thank my advisor Dr. Ehsan Vahidi for his time and support in this study. Also, the Department of Mining and Metallurgical Engineering for the opportunity to make this research happen. Dr. Rasoul for his help with the design of experiments and the staff and faculty that helped me through my masters at the University of Nevada, Reno. Lastly, thanks to my committee members Dr. Carl Nesbitt and Dr. Dev Chidambaram for taking their time to guide me through this research.

Thanks to my family and friends that motivated me to keep on putting all my effort to this study. I would have not made it without you.

Table of Contents

List of tables

List of Figures

1.   Introduction

Lithium production has increased almost three times over the last decade and therefore the number of spent lithium-ion batteries (LIB) has multiplied as well (Tabelin et al., 2021). The United States produces lithium in small amounts but is not a producer of any of the other raw materials needed for the manufacturing process of LIBs. Thus, the main strategy in the US is to implement recycling programs to tackle its demand for key materials (Kane, 2019). As the demand for LIBs increases, so will the disposal of spent batteries in the solid waste stream, and more batteries will end up in landfills. If failing to get disposed of correctly, LIBs can release toxic chemicals into the environment (Jiang & Zeng, 2015).

Figure 1 shows how the use of lithium-ion batteries will grow in each sector. Passenger electric vehicles are the category that has the bigger projection followed up by commercial vehicles, stationary storage, consumer electronics, and E-buses. By the year 2030, the world will need almost 2000 gigawatt-hours to power all these products.
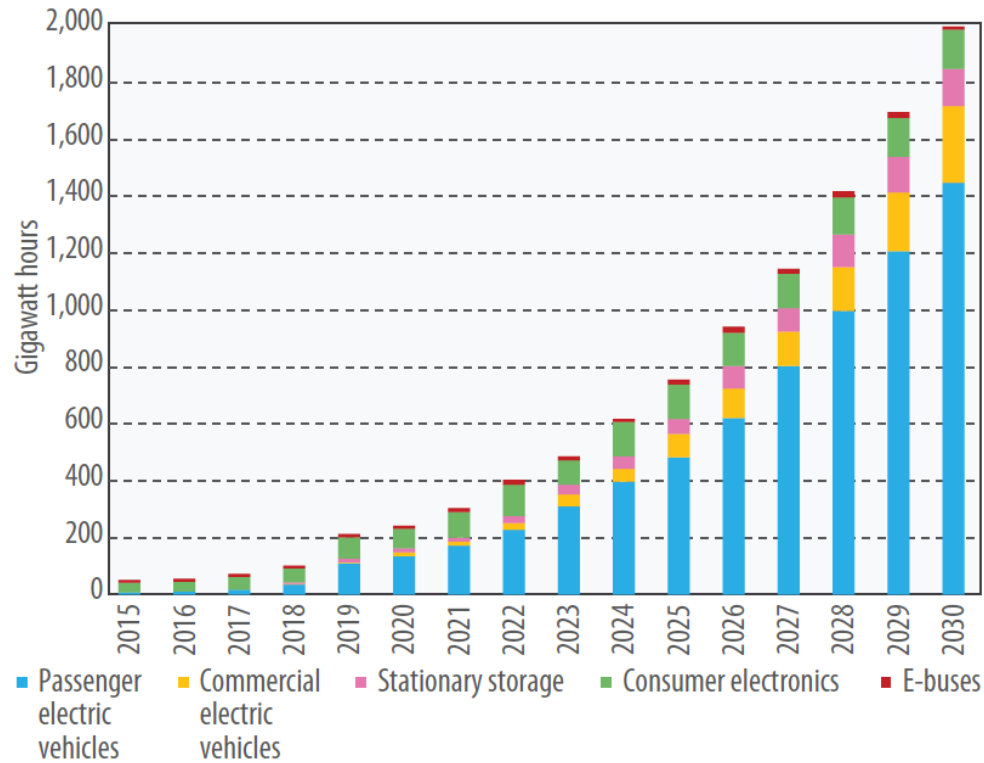
Figure 1 Uses of lithium-ion batteries in the world 2015-2030 (Wang, n.d.)

Sales for EVs are soaring thanks to how available EVs are for people around the world (IEA, 2020). It is estimated that by 2030, the amount of EVs that will be sold in the world will generate a lithium and cobalt demand of 3.4 and 1.7 times, respectively compared to 2017 (Jones et al., 2020). Thus, LIBs have become the future of electric power generation.

Through the years many ways of recycling the critical and strategic elements inside them have emerged. From these critical and strategic mineral commodities, cobalt (Co), lithium (Li), manganese (Mn), and graphite are identified as critical materials used in the production of LIB cathodes to be utilized in electric vehicles and other electronic devices (USGS, 2020). In addition, nickel (Ni) is considered a strategic material for the future

production of LIBs as it helps deliver higher energy density and greater storage capacity at a lower cost (Nickel Institute, 2020). LIBs are composed of a metallic layer, membrane separator, cathode materials, aluminum foil, anode materials, copper foil, and electrolytes. The cathode materials are the ones that are of interest for the recycling of LIBs that are known to be $LiCoO_2$ (LCO), $LiMn_2O_4$ (LMO), $LiFePO_4$ (LFP), and Li_2TiO_3 (LTO) (Zhang et al., 2019). $LiNiCoMnO_2$ (NMC) is a commonly used cathode composition in today's industry (Busà et al., 2021). LIBs are manufactured by a number of different powders with different compositions. The following table shows the type of batteries and the weight percent of each element inside the powders. Figure 2 shows the current trends in powder chemistries used in the lithium-ion battery industry. In 2017 the most common type of battery chemistry was LFP with 38% of the batteries being produced with this chemistry. It is projected that by 2025 the most popular battery chemistry will be NMC with almost 70% of the battery manufacturing containing this chemistry.
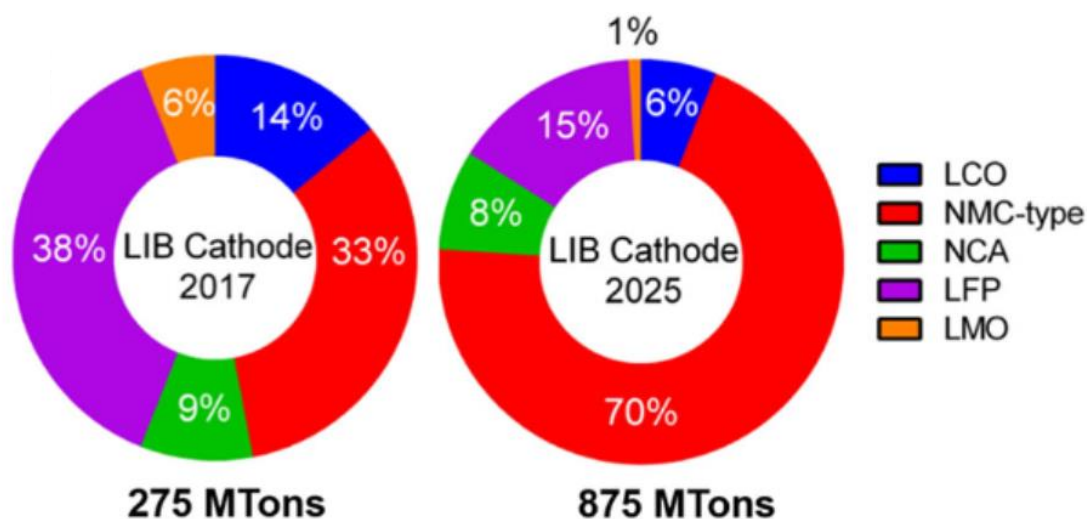
Figure 2 Projected cathode chemistry shift (Or et al, 2019)

Among the most used types of cathode materials, NMC, LFP, and LTO have their own advantages and disadvantages. NMC's main advantages are the higher density, safety, and stability they provide when the right ratio of metals is used. On the other hand, NMC powders can be pricey and have a lower lifetime. When a high content of nickel is used, the battery becomes unstable and is more prone to ignition. The main advantage of LFP powders is that they are more affordable than NMC and LTO powders. LFP powder's affordability comes at a cost of having lower energy density. Finally, LTO powder's main advantages are that they are more stable and have a longer lifetime. LTO powders have lower energy density than NMC or LFP powders and therefore, they have a higher cost but are more robust (Jehle, 2021).

When mixed correctly, NMC cathode powders have proven to be more stable and able to have a larger energy density than the other types of powders. The most common types of NMC powders are 811, 333, or 523 (Yabuuchi & Ohzuku, 2003). These numbers mean that the ratio of nickel, manganese, and cobalt is 8:1:1, 3:3:3, or 5:2:3, respectively. Depending on the battery manufacturer, the ratio of these three main elements might vary to adjust to the primary needs of the cell. It has been proven that by having higher nickel content in a battery, the capacity of the battery will increase but the battery would become unstable (Nitta et al., 2015). On the other hand, having a higher concentration of cobalt or manganese in a battery cell would increase the cycles of charge and discharge. In addition it will provide more stability to the battery but would decrease the capacity of the battery (Stan et al., 2014). In this study, NMC 523 was selected because the nickel content is not too high, and the cobalt and manganese content, are increased from the usual NMC 811.

Thus, once the battery materials need to be recovered, the ratio will have better cycle life and will be safer to use.

Most of the critical metals needed to manufacture a lithium-ion battery come from other countries. The United States' lithium production is limited to a brine deposit located in Nevada and therefore, this country needs to rely upon other countries' production. Approximately, 44% of the lithium reserves are located in Chile (Ore et al., 2021). The Democratic Republic of Congo (DRC) accounted for almost 60% of the world's production of cobalt in the world (USGS, 2018). South Africa accounts for almost 33% of the production of manganese, while China produces 67% of the graphite. Nickel comes in small quantities from several different countries. Among the main sources of nickel, the Philippines produces 11% of this metal (M. Chen et al., 2019). Even though the production of cathode powders is dominated by foreign markets, refinement of the materials used in electric batteries occurs mainly in China (Xu et al., 2020).

In the United States, the only known domestic reserves of the mentioned critical and strategic metals are known to be either low grade or difficult to mine (USDOE, 2020). Given that the United States is globally competitive in the downstream supply chain in cell and battery pack manufacturing, this country is one of the main buyers of the refined cathode powders produced by other countries. In 2019, the United States imported most of the critical and strategic metals to use in LIBs from other countries. Having a dependency to manufacture LIBs has a huge impact on the prices and puts recycling in the spotlight (USDOE, 2020).

Therefore, it is imperative to develop means of recovering critical and strategic materials from defective and spent powders to meet growing future demand. To recover valuable metals such as lithium, cobalt, manganese, and nickel from spent Li-ion batteries, some typical hydrometallurgical and pyrometallurgical processes have been proposed in the literature. A pyrometallurgical approach to LIB's recycling entails the use of heat to form alloys from smelted spent LIBs. Even though it is a straightforward process, there are a lot of disadvantages when using this approach (Meshram et al., 2020). The main disadvantage is the cost of smelting due to the need for high temperatures. Also, when smelting an entire cell, there are many impurities that melt with the valuable metals, and further purification steps will be needed to produce pure metallic elements (Assefi et al., 2020). Nowadays, hydrometallurgical processes are applied, and the mentioned critical elements will be recovered from LIBs with the use of inorganic acids such as nitric acid (HNO_3) (Guan et al., 2017), hydrochloric acid (HCl) (Guo et al., 2016), and sulfuric acid (H_2SO_4) (Urbańska, 2020). The use of inorganic acids in LIBs recycling makes the process faster and efficient but the waste material generated after the leaching of the critical elements creates negative environmental impacts (Ekberg & Petranikova, 2015).

Table 1 shows different parameters found in the literature, it can be perceived that optimal conditions have only been optimized for a specific metal or metals. Previous investigations showing an optimized condition for all critical metals were hard to find or non-existent. Even if there were optimized conditions none of them explained the environmental impact that it would have. Taken together, the results of this investigation will greatly improve our ability to recover critical and strategic materials from defective and spent batteries, which, in turn, will enable us to answer the growing demand for the

critical and strategic elements, to decrease the demand for raw materials, and to avoid spent batteries from entering the solid waste stream (Gaines, 2018).

An example of this is by looking at the results from the literature review. For sulfuric acid, there are two publications where the authors only looked at the optimized conditions for two or three of the critical metals. Then the other authors did look at the optimization of the four critical metals. All the authors combined did not analyze what environmental impact their optimized condition will have. For example, two authors claimed that they can reach more than ninety percent recovery of lithium (He et al. 2018 and Diaz et al. 2020). The first of the previously mentioned experiments requires a higher dosage of H_2O_2 while the other needs a higher L/S ratio which would mean more water needs to be added to the system. These two optimized conditions yield a high recovery of metal, but they do not analyze how detrimental would be to consume more reagents or to need more water in the system. Similarly for the other two inorganic acids analyzed in this research, researchers often show optimized conditions to get most of the metal extraction but do not take into consideration the environmental impact.

In this study, the optimized conditions were generated using statistical software that took into consideration all the inputs and maximized the outputs which were the metal recoveries for all four critical metals. After optimizing the conditions for each inorganic acid, a deep and comprehensive life cycle assessment was conducted to determine the best acid that had a better environmental performance. It is important to understand the design of experiments software and the statistical optimization that was used in this research and the benefits it provides to find the best parameters of the experiments.

Table 1. Literature review of the leaching parameters with inorganic acids.

Leaching Agent	Concentration (mol/l)	Temperature (°C)	Time (min)	(g/l)	Co-additive (vol %)	Efficiency	Source
H_2SO_4	0.57	75	120	6	Fe ions 6 g/l	Li: 92.67 Co: 98.91	(Ghassa et al., 2020)
H_2SO_4	1	60	12 hrs		H_2O_2 1%	Ni: 96.13, Co: 96.83, Mn: 97.45	(He et al., 2018)
H_2SO_4	1	40	60	40	H_2O_2 1%	Li: 99.7, Ni:99.7, Co:99.7, Mn: 99.7	(He et al., 2017)
H_2SO_4	1	95	240	50	H_2O_2 5%	Li:93.4, Ni: 96.3, Co: 79.2, Mn: 84.6	(Meshram et al., 2016)
H_2SO_4	2	80	60	50	H_2O_2 2%	Li: 81, Ni: 98.7, Co: 98.2, Mn: 97.1	(X. Chen et al., 2015)
H_2SO_4	2 M	60	120	240		Li, Co, Mn, Ni: 96+	(Diaz et al., 2020)
H_2SO_4	2	80	60	50	Hydrazine sulfate 30g/L	Li: 97, Ni: 96, Co: 95, Mn:86	(Yang et al., 2020)
HCl	1	90	120	25	H_2O_2 20%	Li: 94.9, Ni: 94.4, Co: 94.5, Mn: 95.5	(Gu et al., 2020)
HCl	3	80	90	20	H_2O_2 10:1	Li:99.4	(Guo et al., 2016)
HCl	1:03	250	60	30	chlorinated polyvinyl chloride	Li: 98.71, Co: 97.69	(Nshizirungu et al., 2020)
HNO_3	1	75	60	10	H_2O_2 1.7%	Li: 99 Co: 99	(Lee & Rhee, 2002)
HNO_3	2	60	180	10	Na_2CO_3	Li:73.1	(Wu et al., 2021)

2.   Experimental

2.1 Selection of reagents for leaching experiments

Researchers have been studying multiple leaching reagents to narrow down the most efficient inorganic acids to be used in the leaching process. Nitric acid (HNO_3 69%,) hydrochloric acid (HCl 39%), and sulfuric acid (H_2SO_4 97%) were used as the leaching agents in the recovery of valuable metals from NMC 523 cathodic powder for this thesis. Hydrogen peroxide (H_2O_2) has been the most effective co-additive when combined with the previously mentioned inorganic acids by assisting the reaction to break the bonds between cobalt and oxygen and overall promoting the dissolution of the ions (Lin, 2020). Hydrogen peroxide has been known to improve the metal recoveries for lithium, cobalt, manganese, and nickel to more than 90%.

2.2 Sample preparation

The cathode powders were purchased from MTI corporation and the main component is $LiNiCoMnO_2$ where the Ni:Co:Mn ratio is 5:2:3. The percentage of lithium is 7-8% and Ni+Co+Mn is >58%. One gram of the cathode powder was used for all experiments. Before measuring each sample, the bottle was well shaken to homogenize the powder.

2.3 Analytical method

To calculate the recoveries of the leaching efficiencies of the elements, atomic absorption spectroscopy (AAS) was used. Based on the initial concentrations and the AAS results, the recoveries of lithium, nickel, cobalt, and manganese were calculated using the following formula:

$$\text{Metal recovery (\%)} = \frac{Cf \times \text{Dilution}}{Ci} \times 100$$

Where Cf is the final concentration in ppm read by the AAS and Ci is the initial concentration calculated using:

$$\text{Initial concentration (ppm)} = \frac{P \times 1000 \times M\%}{\dfrac{V}{1000}}$$

Where P is the powder weight used for the experiment in grams, M% is the metal percentage in the powder and V is the volume in ml used for the experiment.

2.4 Leaching experiments

The experiments were performed using one gram of powder, and the volume and the molarity changed based on the design of experiments for each acid. Figure 3 shows the experimental apparatus for conducting leaching experiments at low and high temperatures. The temperature was measured using both an electronic thermometer and a glass thermometer. The electronic thermometer was used for low temperature and the glass thermometer was used for the high-temperature experiments. After every experiment was completed a round nylon filter paper was used to prevent any undissolved solids from entering the collected solution. Even the fully dissolved experiments were filtered using a whatman grade 1 qualitative filter paper.

Figure 3. Low temperature (left) and high temperature (right) experiment set up.

Figure 4 shows the most common stream to obtain NMC powders It is important to point out that NMC powder can be obtained either from the dismantling of spent lithium-ion batteries or from defective NMC powders that did not meet the quality standard prior to manufacturing the battery.
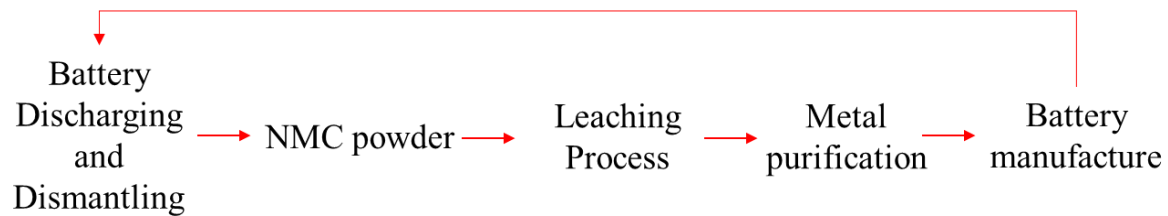
Figure 4. Flow diagram of general recycling process for lithium-ion batteries.

3.   Design of Experiments

The statistical design for this research was made using Design Expert V.10. Using data from the literature the software was able to generate the calculations and modeling to optimize the outputs. The molarity (M), temperature (°C), time (min), solid to liquid ratio (L/S) and H_2O_2 (v/v %) were the parameters investigated in this design. The optimized responses were lithium, cobalt, manganese, and nickel recoveries. The temperature was set to not exceed 70 degrees Celsius to avoid hydrogen peroxide decomposition and to match the temperatures used in the industry.

Response surface methodology (RSM) plots were generated to optimize the parameters in each of the designs. This RSM plots approximate the responses of each of the variables introduced and show the interactions and possible behavior for each of the metal recovery responses (Sarabia & Ortiz, 2009). The color change makes it easy to identify the optimized point in each plot. The red color signifies the maximum outputs, while the green/blue colors on the plots represent points of minimum output for each of the responses. Some of the diagrams show red and pink dots that represent the design points that were above the predicted value and the points that were below the predicted value of the design respectively. These dots represent statistical error and are considered outliers.

The software generates grids in each of the plots that represent all combinations of design choices taking into consideration the values that were input into it. This design of experiments reduced the number of experiments that needed to be performed in each of the optimizations while getting statistically accurate results (Aydar, 2018). For this design, a polynomial approximation and a central composite design was used to calculate what

happens in between data points to generate the RSM for each scenario. The software generated 30 experiments that needed to be experimentally performed and analyzed to then generate its own predictions for the intermediate point using the previously mentioned methods. Combining the design of experiments and the RSM demonstrates statistical significance to the results, and it helps predict the optimal conditions to maximize all four metal recoveries in our study. The desirability plots show one of the possible one hundred solutions for this design. The solution with the highest desirability was chosen and replicated as validation for the design of each of the acids. The higher the desirability means that is how close the prediction of the model was to the actual values of the results that were performed in the laboratory.

3.1 H_2SO_4

Table 2 shows the order that the experiments were carried out changing the parameters to optimize the responses mentioned previously. To minimize error the software randomizes the order of the experiments and suggests the run order to be followed to give more accuracy to the model.

Table 2. Design of experiments and responses for the leaching using H_2SO_4.

Std	Run	A: Concentration	B: Temperature	C: Time	D: L/S	E:H_2O_2 Conc.	Li Recovery	Co Recovery	Mn Recovery	Ni Recovery
		M	°C	min	l/g	%	%	%	%	%
14	1	2.5	25	80	0.1	0	82	39	35	49
26	2	1.5	47.5	50	0.067	1.25	97	69	59	94
10	3	2.5	25	20	0.1	1	90	70	53	95
13	4	0.5	25	80	0.1	1	84	66	41	89
4	5	2.5	70	20	0.033	1	90	89	59	80
29	6	1.5	47.5	50	0.067	0.5	99	70	59	92
25	7	1.5	47.5	50	0.067	0	82	41	23	57
2	8	2.5	25	20	0.033	0	63	27	21	35
7	9	0.5	70	80	0.033	1	79	87	47	81
17	10	0.01	47.5	50	0.067	0.5	~~27~~	~~15~~	~~20~~	~~33~~
15	11	0.5	70	80	0.1	0	78	41	23	92
16	12	2.5	70	80	0.1	1	86	84	59	76
21	13	1.5	47.5	5	0.067	0.5	84	67	62	86
20	14	1.5	81	50	0.067	0.5	82	70	47	77
6	15	2.5	25	80	0.033	1	82	79	55	70
12	16	2.5	70	20	0.1	0	89	29	53	33
8	17	2.5	70	80	0.033	0	95	24	16	39
24	18	1.5	47.5	50	0.116	0.5	98	65	62	89
3	19	0.5	70	20	0.033	0	66	23	23	37
5	20	0.5	25	80	0.033	0	53	17	20	31
23	21	1.5	47.5	50	0.016	0.5	86	78	57	72
11	22	0.5	70	20	0.1	1	88	63	70	76
18	23	3	47.5	50	0.067	0.5	98	79	70	90
9	24	0.5	25	20	0.1	0	31	16	6	16
19	25	1.5	14	50	0.067	0.5	83	66	55	83
30	26	1.5	47.5	50	0.067	0.5	96	67	82	94
27	27	1.5	47.5	50	0.067	0.5	100	79	66	94
22	28	1.5	47.5	95	0.067	0.5	97	72	70	97
28	29	1.5	47.5	50	0.067	0.5	101	84	66	97
1	30	0.5	25	20	0.033	1	35	23	20	33

3.1.1 Results and discussion

The accuracy of the models proposed in this study was confirmed using ANOVA tables for each inorganic acid and can be found in the supporting information. Figure 5 show the 3D surface plots for sulfuric acid. From these figures, for each response the optimal conditions vary for each element.
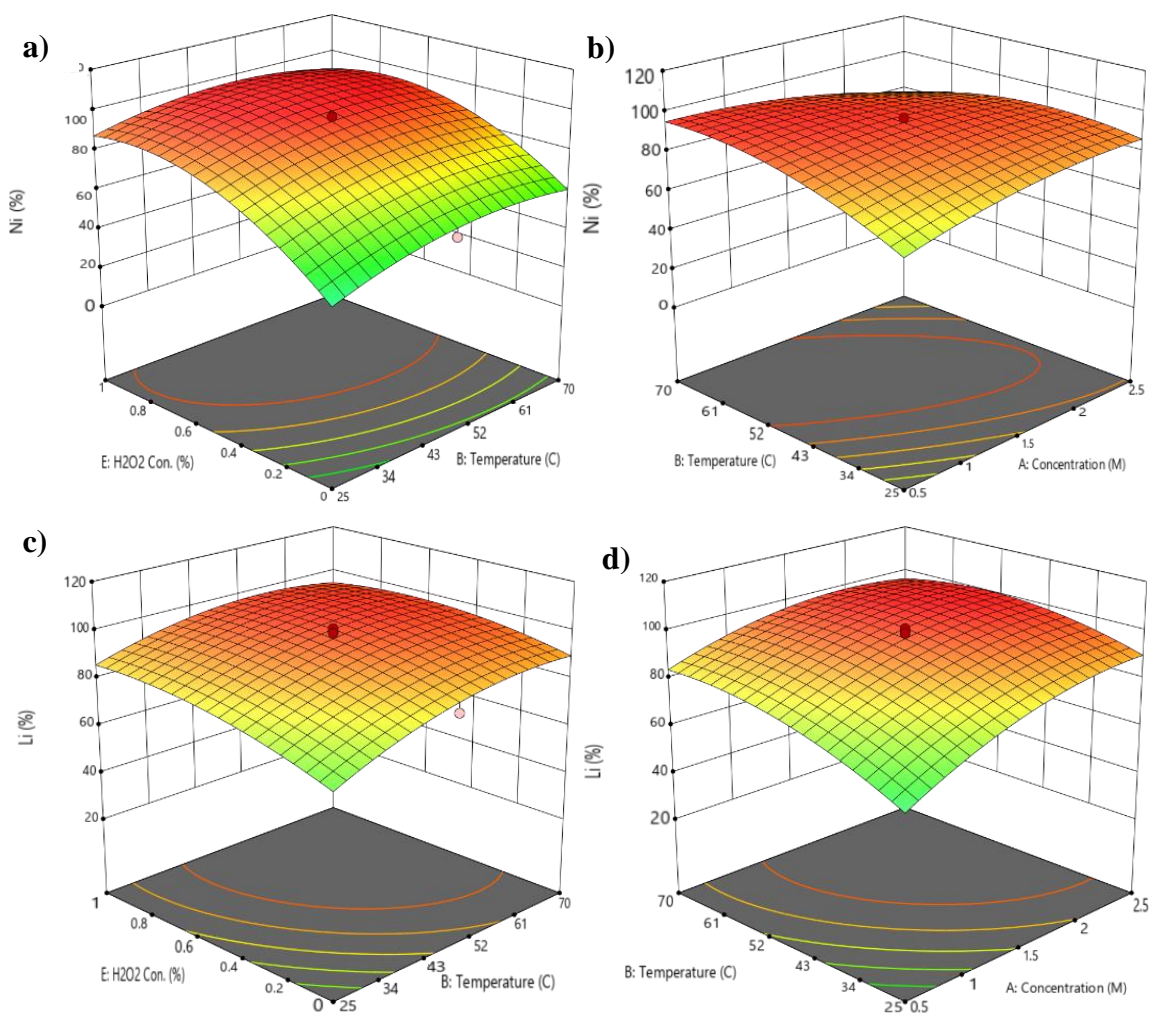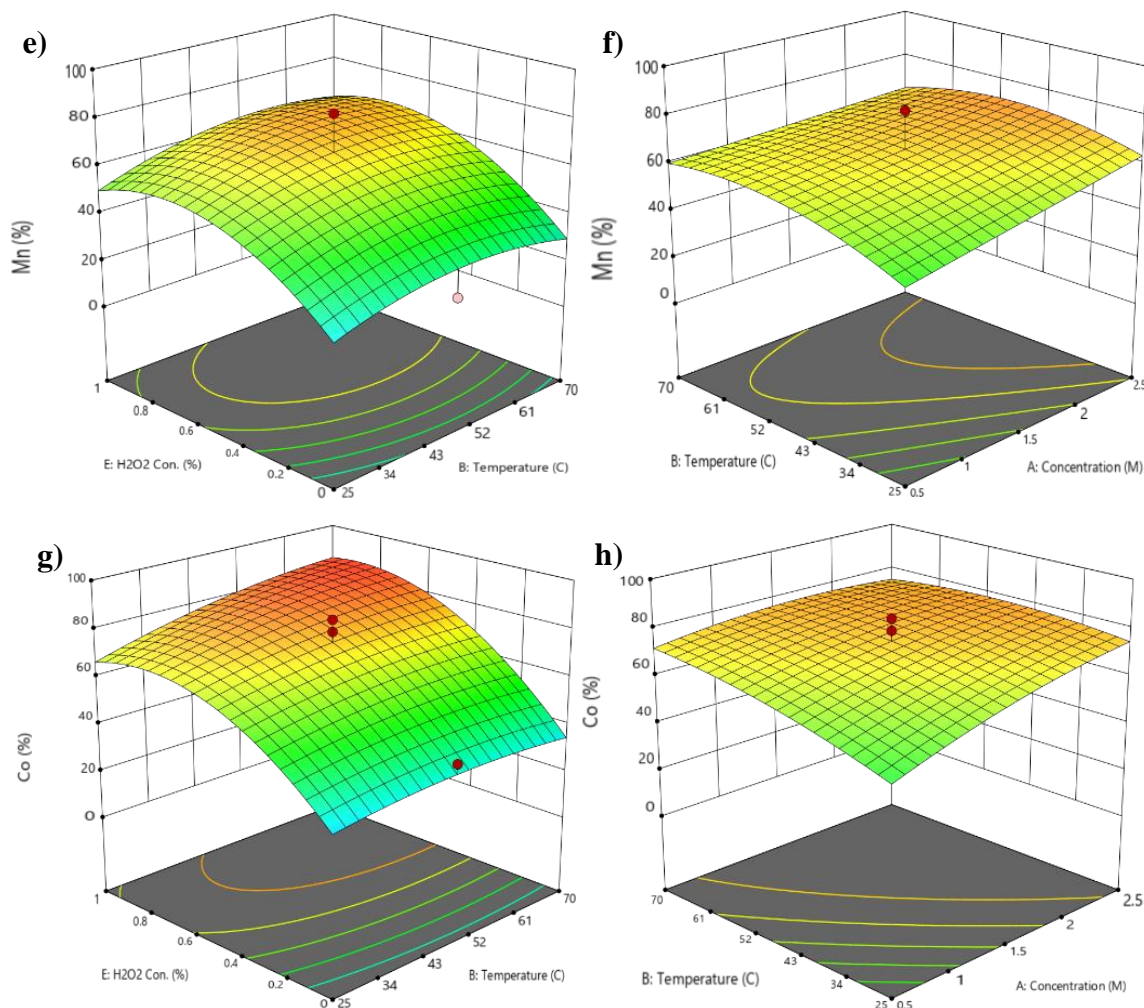
Figure 5. 3D surface plots for H_2SO_4. *A***)** Ni recovery (%) as a function H_2O_2 conc. (%) and temperature (ºC), **b)** Ni recovery (%) as a function of temperature (ºC) and concentration (M), **c)** Li recovery (%) as a function H_2O_2 conc. (%) and temperature (ºC), **d)** Li recovery (%) as a function of temperature (ºC) and concentration (M), **e)** Mn recovery (%) as a function H_2O_2 conc. (%) and temperature (ºC), **f)** Mn recovery (%) as a function of temperature (ºC) and concentration (M), **g)** Co recovery (%) as a function H_2O_2 conc. (%) and temperature (ºC), **h)** Co recovery (%) as a function of temperature (ºC) and concentration (M).

From the RSMs generated for H_2SO_4, Ni recovery (%) is maximum when H_2O_2 conc. (%) is between 0.6 and 0.4 and temperature is between 43 and 52ºC (Figure 5a), Ni recovery (%) is maximum when the temperature is above 52ºC and the concentration is below 2 M (Figure 5b), Li recovery (%) is maximum when the H_2O_2 conc. (%) is between

0.6 and 0.4 and temperature is between 43 and 52ºC (Figure 5c), Li recovery (%) is maximum when the temperature is closer to 52ºC and the concentration is higher than 1.5 (Figure 5d) and Co recovery (%) is maximum when the H_2O_2 conc. (%) is above 0.6 and temperature is above 52ºC (Figure 5g). For all the other RSMs, there are not clear maximum or minimums for the corresponding outputs which can be concluded that those parameters do not directly affect the response of the model. For example, in Figure 5h, the surface plot does not show a steep peak and the overall surface looks flat which can be concluded from this figure that as the temperature and concentration increases or decreases the Co recovery is not affected. This same trend can be observed for figures 5e and 5f, even though these two figures have more curvature the maximum points are hard to identify.

Figure 6 shows the optimal conditions for sulfuric acid and the transformation of the surface model when increasing or decreasing the parameter limits. Also, Figure 4 shows that desirability on this model is 0.988 which means that the calculated parameters are 98.8% close to the ideal optimum conditions for each of the individual responses obtained experimentally in this study

0.5	2.5
A:Concentration = 1.96684	

25	70
B:Temperature = 69.9893	

20	80
C:Time = 20.0083	

0.03333	0.1
D: L/S = 0.0910527	

o	1
E:H2O2 Con. = 0.956647	

27	101
Li = 105.652	

15	89
Co = 85.4843	

6	82
Mn = 82	

16	97
Ni = 96.9998	

Desirability = 0.988
Solution 1 out of 100
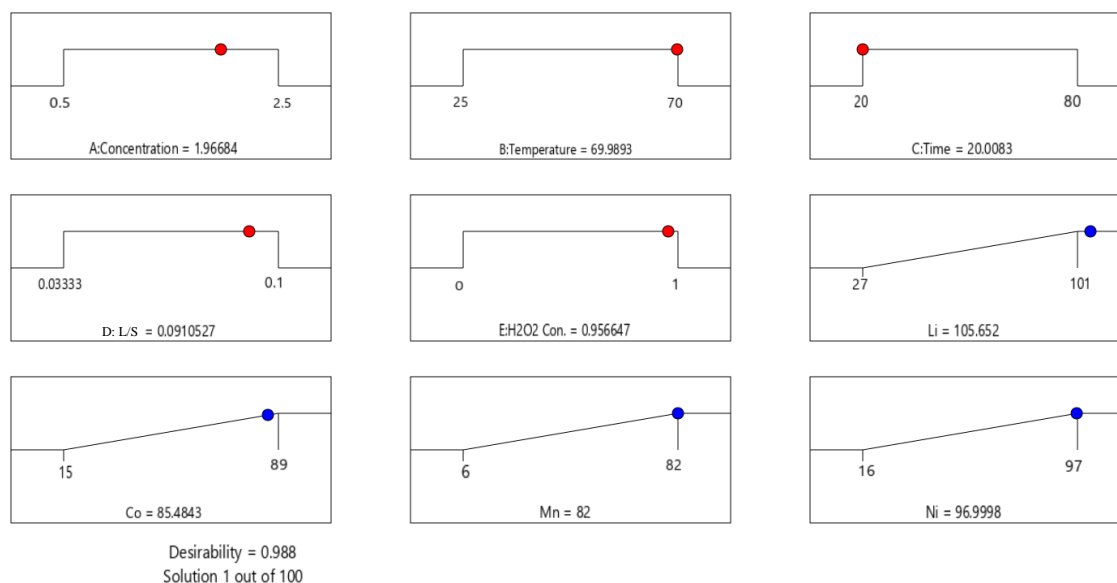
Figure **6***.* Desirability values of all responses in optimum conditions: 1.97 M, 69.99ºC, 20 min, L/S:0.091 and 0.957 H_2O_2 con c.

3.1.2 Effective Parameters in Leaching

Leaching agent H_2SO_4 can effectively dissolve the major metals in the cathode powder. Also, the H_2O_2 con. (v/v%) plays an important role as an oxidative reagent to accelerate the reaction. It has been shown that the adequate molarity and H_2O_2 con. (v/v%) must be 1.96 and 0.957 respectively to optimize the metal recovery.

Temperature 69ºC has been proven to be the optimal temperature to maximize the solubility of the metals and therefore reach a maximum dissolution to obtain the best metal recovery. Lower temperatures showed to decrease the metal recovery. On the other hand, high temperatures are proven to not improve the recoveries by much and can be concluded to be a waste of energy to reach those temperatures.

Time from all the inorganic acids in this study sulfuric acid showed that it needs less amount time to reach full dissolution while getting the best responses. 20 min is sufficient time and therefore less energy is consumed when compared to other acids.

L/S ratio Optimal solid to liquid ratio has been determined to be an important parameter in this study. Keeping the ratio at 0.091 has shown to get optimal responses. Lowering the L/S ratio decreases the recovery of some of the responses.

3.2 HCl

Table 3 shows the design of experiments that was generated for hydrochloric acid and the responses that were obtained from each experiment.

Table 3. Design of experiments and responses for the leaching using HCl.

Std	Run	A: Concentration	B: Temperature	C: Time	D: L/S	E: H_2O_2 Conc.	Li Recovery	Co Recovery	Mn Recovery	Ni Recovery
		M	°C	min	l/g	%	%	%	%	%
11	1	0.5	70	20	0.1	1	91	100	79	92
1	2	0.5	25	20	0.033	1	41	44	69	98
6	3	2	25	90	0.033	1	81	88	100	100
29	4	1.25	47.5	55	0.067	0.5	94	88	57	46
15	5	0.5	70	90	0.1	0	93	46	41	45
14	6	2	25	90	0.1	0	73	45	28	52
18	7	2.37	47.5	55	0.067	0.5	93	100	57	42
23	8	1.25	47.5	55	0.017	0.5	67	54	64	72
28	9	1.25	47.5	55	0.067	0.5	91	74	80	92
7	10	0.5	70	90	0.033	1	56	39	38	42
3	11	0.5	70	20	0.033	0	61	37	37	40
17	12	0.13	47.5	55	0.067	0.5	34	26	9	42
12	13	2	70	20	0.1	0	86	74	79	80
2	14	2	25	20	0.033	0	62	37	100	17
26	15	1.25	47.5	55	0.067	1.3	96	100	94	100
27	16	1.25	47.5	55	0.067	0.5	96	100	80	69
19	17	1.25	20	55	0.067	0.5	87	93	74	73
10	18	2	25	20	0.1	1	89	100	10	11
20	19	1.25	81	55	0.067	0.5	90	90	85	88
21	20	1.25	47.5	10	0.067	0.5	90	100	41	42
16	21	2	70	90	0.1	1	92	83	93	100
9	22	0.5	25	20	0.1	0	40	29	7	11
8	23	2	70	90	0.033	0	82	94	93	100
24	24	1.25	47.5	55	0.116	0.5	98	100	20	33
4	25	2	70	20	0.033	1	86	86	77	88
13	26	0.5	25	90	0.1	1	89	100	28	46
5	27	0.5	25	90	0.033	0	52	32	2	6
22	28	1.25	47.5	107	0.067	0.5	100	82	69	73
25	29	1.25	47.5	55	0.067	0	83	51	44	57
30	30	1.25	47.5	55	0.067	0.5	94	55	55	61

3.2.1 Results and discussion

The ANOVA tables for hydrochloric acid can be found in the supporting information. Figure 7 shows all the possible combinations of inputs and the corresponding response that yield the best conditions for HCl.
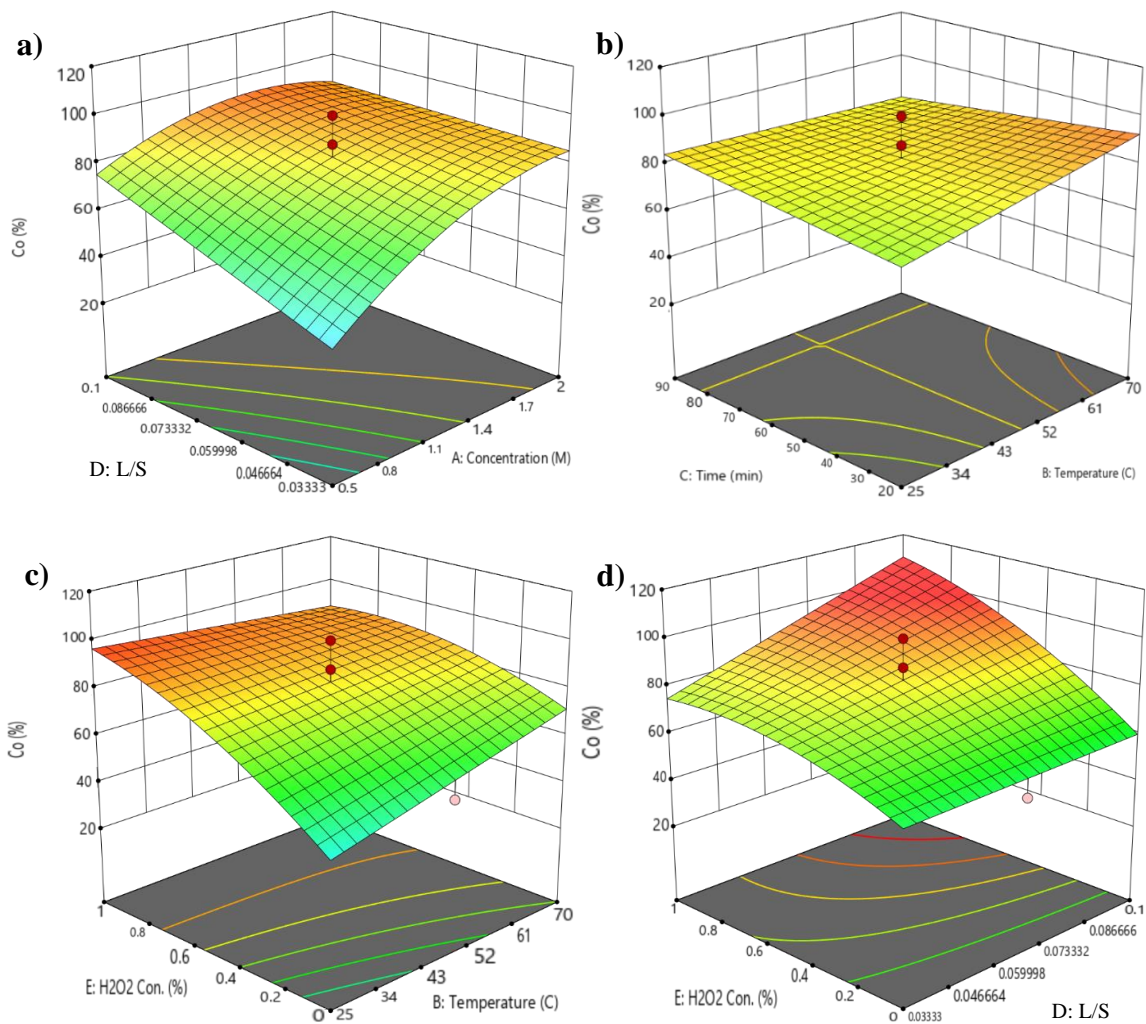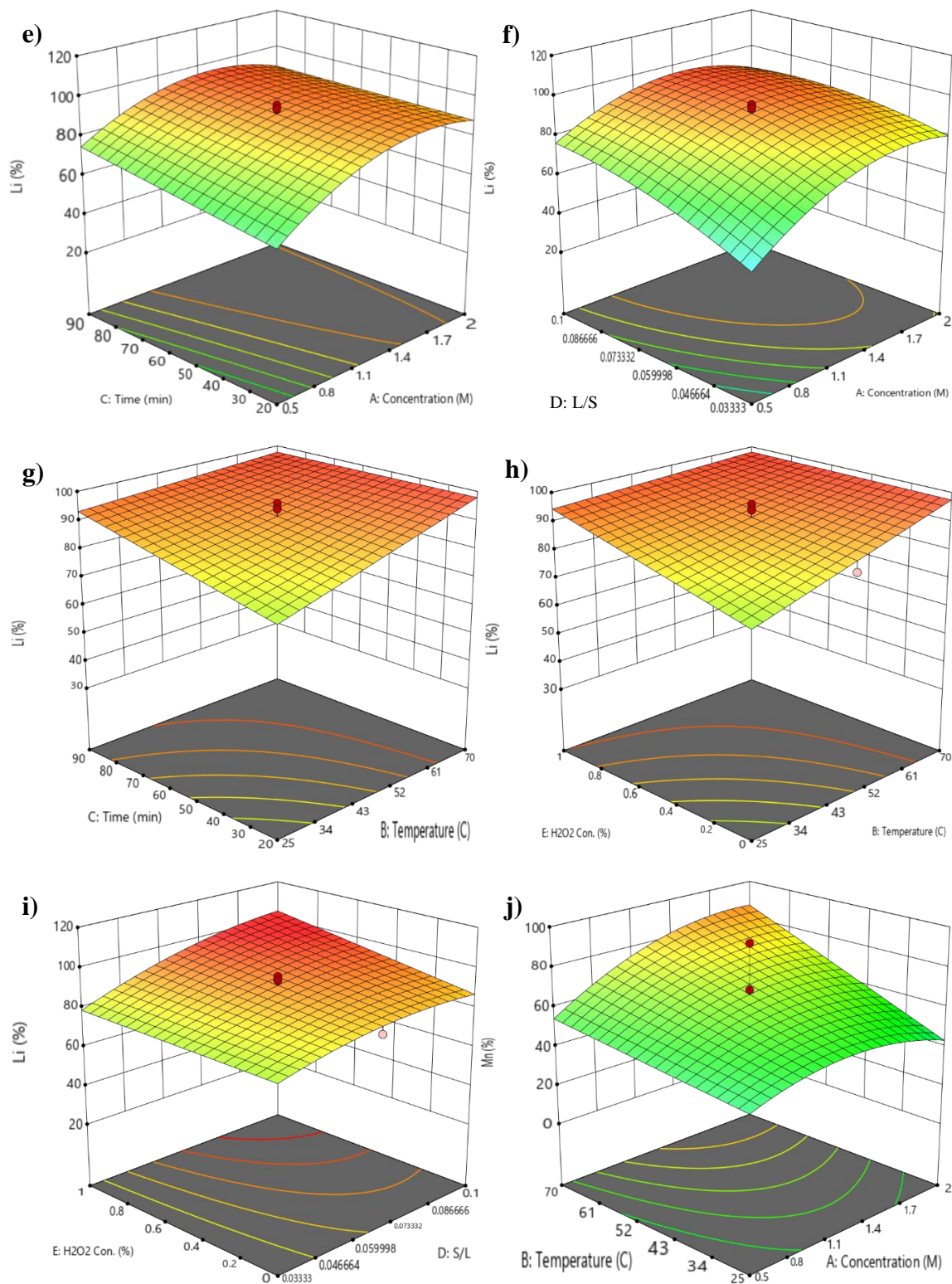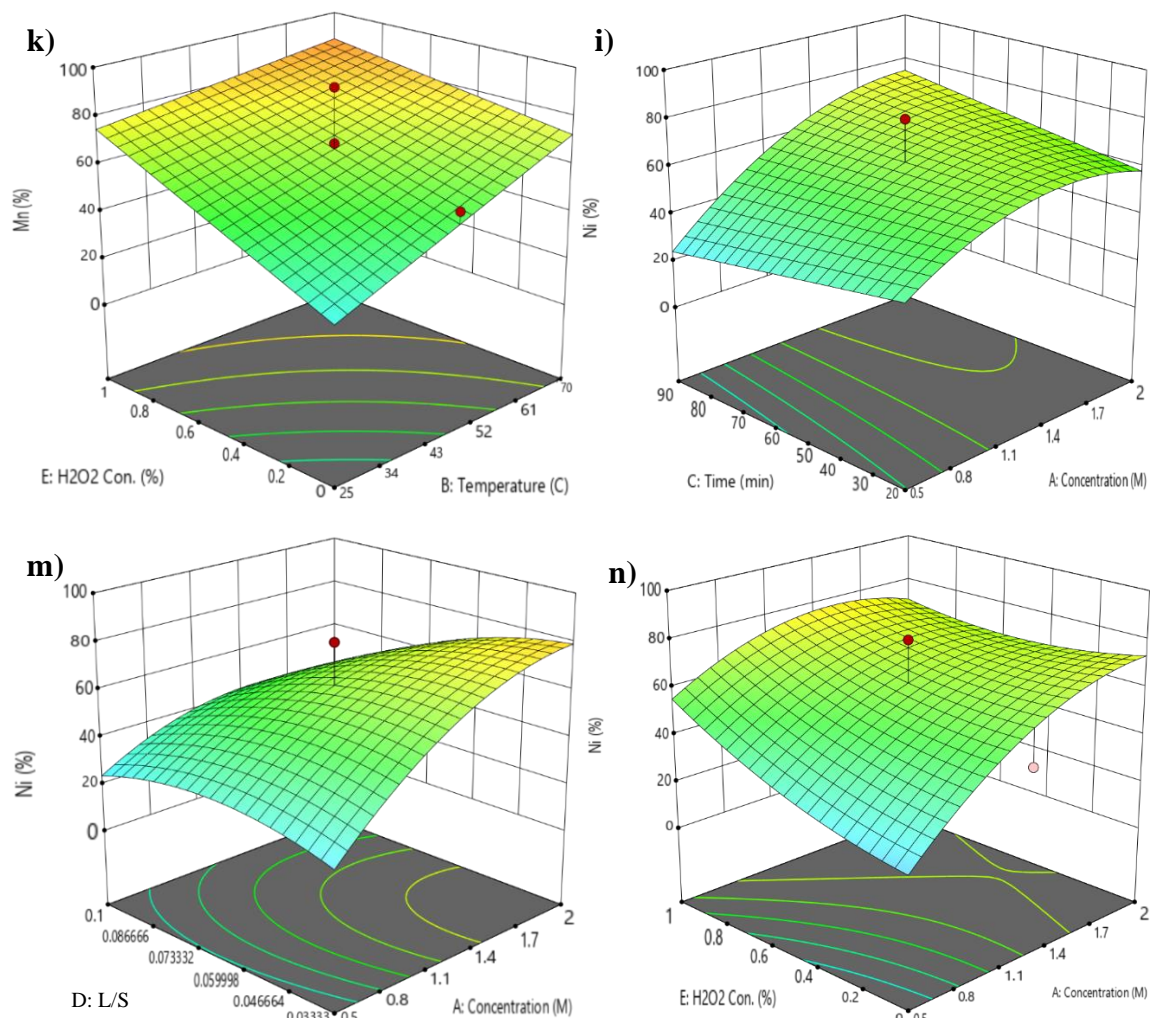
Figure 7. Surface Plots for HCl. a) Co recovery (%) as a function of L/S and concentration (M), **b)** Co recovery (%) as a function of time (min) and temperature (ºC), **c)** Co recovery (%) as a function H$_2$O$_2$ conc. (%) and temperature (ºC), **d)** Co recovery (%) as a function H$_2$O$_2$ conc. (%) and L/S, **e)** Li recovery (%) as a function of time (min) and concentration (M), **f)** Li recovery (%) as a function of L/S and concentration (M), **g)** Li recovery (%) as a function of time (min) and temperature (ºC), **h)** Li recovery (%) as a function H$_2$O$_2$ conc. (%) and temperature (ºC), **i)** Li recovery (%) as a function H$_2$O$_2$ conc. (%) and L/S, **j)** Mn recovery (%) as a function of temperature (ºC) and concentration (M), **k)** Mn recovery (%) as a function H$_2$O$_2$ conc. (%) and temperature (ºC), **l)** Mn recovery (%) as a function of time (min) and concentration (M), **m)** Ni recovery (%) as a function of L/S and concentration (M), **n)** Ni recovery (%) as a function H$_2$O$_2$ conc. (%) and concentration (M).

For the RSMs generated for HCl, Co recovery (%) is maximum when the L/S is higher than 0.07 and the concentration is closer to 1.4 M (Figure 7a). Additionally, Co recovery (%) is maximum when the H_2O_2 conc. increases while the temperature does not play an important role (Figure 7c), Co recovery (%) is maximum when the H_2O_2 conc. (%) and the L/S ratio increase (Figure 5d), Li recovery (%) is maximum when the time (min) is above 60 and the concentration is between 1.4 and 1.7 M (Figure 7e). Furthermore, Li recovery (%) is maximum when the L/S ratio is higher than 0.07 and the concentration is between 1.4 and 1.7 M (Figure 7f), Li recovery (%) is maximum when the H_2O_2 conc. (%) and the L/S ratio increase (Figure 5i), Mn recovery (%) will be maximized when the temperature (ºC), concentration (M), H_2O_2 conc. (%) and the temperature increase (Figures 8j, 8k, and 8l). Ni recovery (%) is maximum when the L/S decreases and the concentration (M) increases (Figure 5m), Ni recovery (%) shows two maximums one when the H_2O_2 conc. (%) is closer to 1 and the concentration is closer to 1.4 M, and the second maximum is when the H_2O_2 conc. (%) is closer to 0 and the concentration is closer to 2 M (Figure 7n). For Figures 7b, 7g and 7h the surface plot is flat which means that if the parameters go high or low, the response will not drastically change.

Figure 8 shows that desirability on this model is 0.985 which means that the calculated parameters are 98.5% close to the ideal optimum conditions obtained experimentally in this study
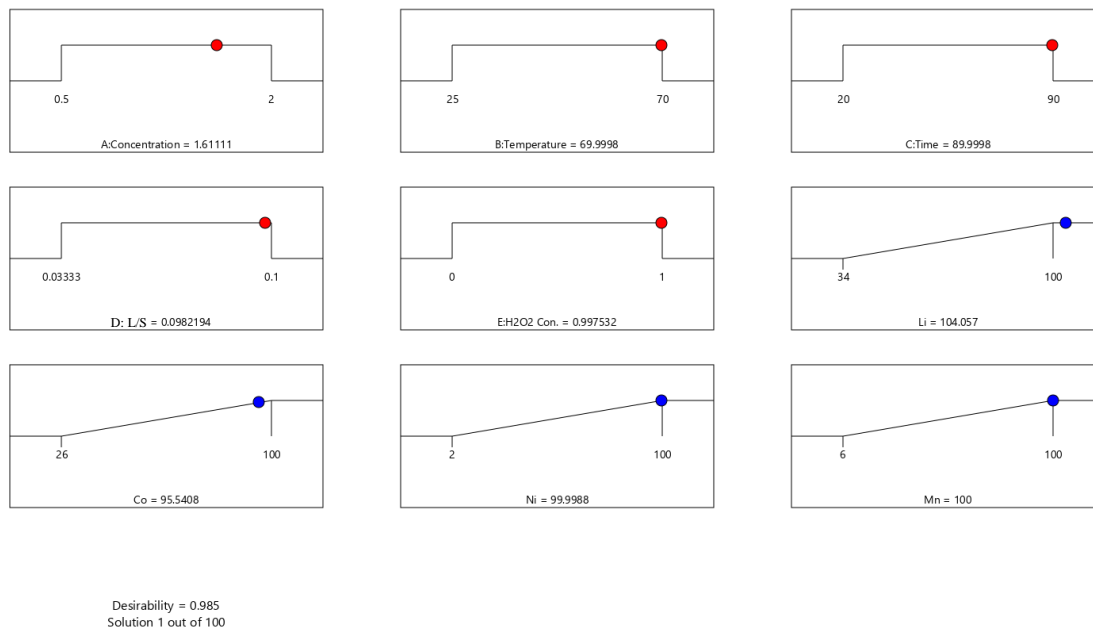
Figure 8. Desirability values of all responses in optimum conditions: 1.611 M, 69.99ºC, 89.9 min, L/S:0.098 and 0.99 H₂O₂ conc.

3.2.2 Effective Parameters in Leaching

Leaching Agent Hydrochloric acid as a leaching agent has proven that it can also yield high recoveries. When added at 1.611 M and mixed with 0.99% H_2O_2 experimentally it can recover 98.75% Li, 95.69% Co, ≈100% Ni and ≈100% Mn

Temperature At 69ºC as the optimal condition is like sulfuric acid. Temperatures below 50ºC show poor recoveries when the concentration is low. Lower temperatures mixed with high leaching agent concentration showed to get high recoveries but using more acid will have an impact down the road especially when dealing with waste and environmental impact.

Time The main difference between HCl and H_2SO_4 is the leaching time. HCl requires almost four times longer than sulfuric acid. When taking into consideration time,

more factors come into play. An example is the electricity cost and efficiency of how much powder can be processed in the industry.

Overall, HCl has similar parameters to sulfuric acid. Leaching time is the biggest difference when taking a close look at this acid. A longer leaching time makes it hard to use in the industry as it becomes inefficient to wait longer when another acid could do the same in less time.

3.3 HNO_3

Table 4 shows the design of experiments that was generated for nitric acid and the responses that were obtained from each experiment.

Table 4. Design of experiments and responses for the leaching using HNO_3.

Std	Run	A: Concentration	B: Temperature	C: Time	D: L/S	E:H_2O_2 Conc.	Li Recovery	Co Recovery	Mn Recovery	Ni Recovery
		M	C	min	l/g	%	%	%	%	%
12	1	1.50	70	20	0.100	0.00	84.44	50.00	68.97	74.71
13	2	0.50	25	90	0.100	0.75	87.78	100.00	68.97	86.21
26	3	1.00	47.5	55	0.067	1.25	94.81	84.48	68.96	99.61
25	4	0.94	47.5	55	0.071	0.00	88.00	37.00	81.00	46.00
22	5	1.00	47.5	107	0.067	0.38	100.00	98.27	50.57	99.61
17	6	0.25	47.5	55	0.068	0.38	57.97	61.33	56.07	97.35
8	7	1.50	70	90	0.033	0.00	77.40	47.98	80.45	82.37
1	8	0.50	25	20	0.033	1.25	38.14	56.03	20.69	47.89
14	9	1.50	25	90	0.100	0.00	54.44	34.48	58.62	80.46
3	10	0.50	70	20	0.033	0.00	58.51	41.09	57.47	40.23
24	11	0.94	47.5	55	0.124	0.38	100.00	89.87	81.32	85.59
21	12	1.00	47.5	10	0.067	0.38	100.00	100.00	82.76	95.78
4	13	1.50	70	20	0.033	1.00	82.58	85.91	85.05	78.54
19	14	1.00	22.1	55	0.067	0.38	67.00	87.00	87.00	87.00
18	15	1.75	47.5	55	0.067	0.38	91.85	86.78	89.65	88.12
9	16	0.50	25	20	0.100	0.00	24.44	34.48	79.31	57.47
27	17	0.94	47.5	55	0.071	0.38	95.47	100.40	83.26	93.87
10	18	1.50	25	20	0.100	0.75	63.33	57.76	55.17	40.23
20	19	1.00	81	55	0.067	0.50	91.11	89.65	87.35	76.63
11	20	0.50	70	20	0.100	1.00	90.00	100.00	75.86	91.95
23	21	0.94	47.5	55	0.017	0.38	75.39	57.99	47.55	31.90
30	22	0.94	47.5	55	0.071	0.38	93.90	89.38	66.12	85.71
29	23	1.00	47.5	55	0.071	0.38	100.00	100.00	93.05	100.00
6	24	1.50	25	90	0.033	0.75	71.84	76.72	50.57	61.30
28	25	1.00	47.5	55	0.071	0.38	98.63	92.44	93.05	93.87
2	26	1.37	25	20	0.037	0.00	23.58	17.03	17.66	16.82
7	27	0.50	70	90	0.033	1.00	58.14	47.70	58.61	63.21
5	28	0.48	25	90	0.034	0.00	42.83	16.02	28.48	37.58
16	29	1.50	70	90	0.050	1.00	87.78	93.53	79.31	80.46
15	30	0.50	70	90	0.050	0.00	70.56	43.10	67.24	68.97

3.3.1 Results and Discussion

The ANOVA tables for nitric acid can be found in the appendix. Figure 9 shows all the possible combinations of inputs and the corresponding response that yield the best conditions for HNO_3. Nitric acid generated more surface plots in the software than sulfuric acid. Therefore, there is more variability in the possible combinations to achieve an optimized response for each of the metals.
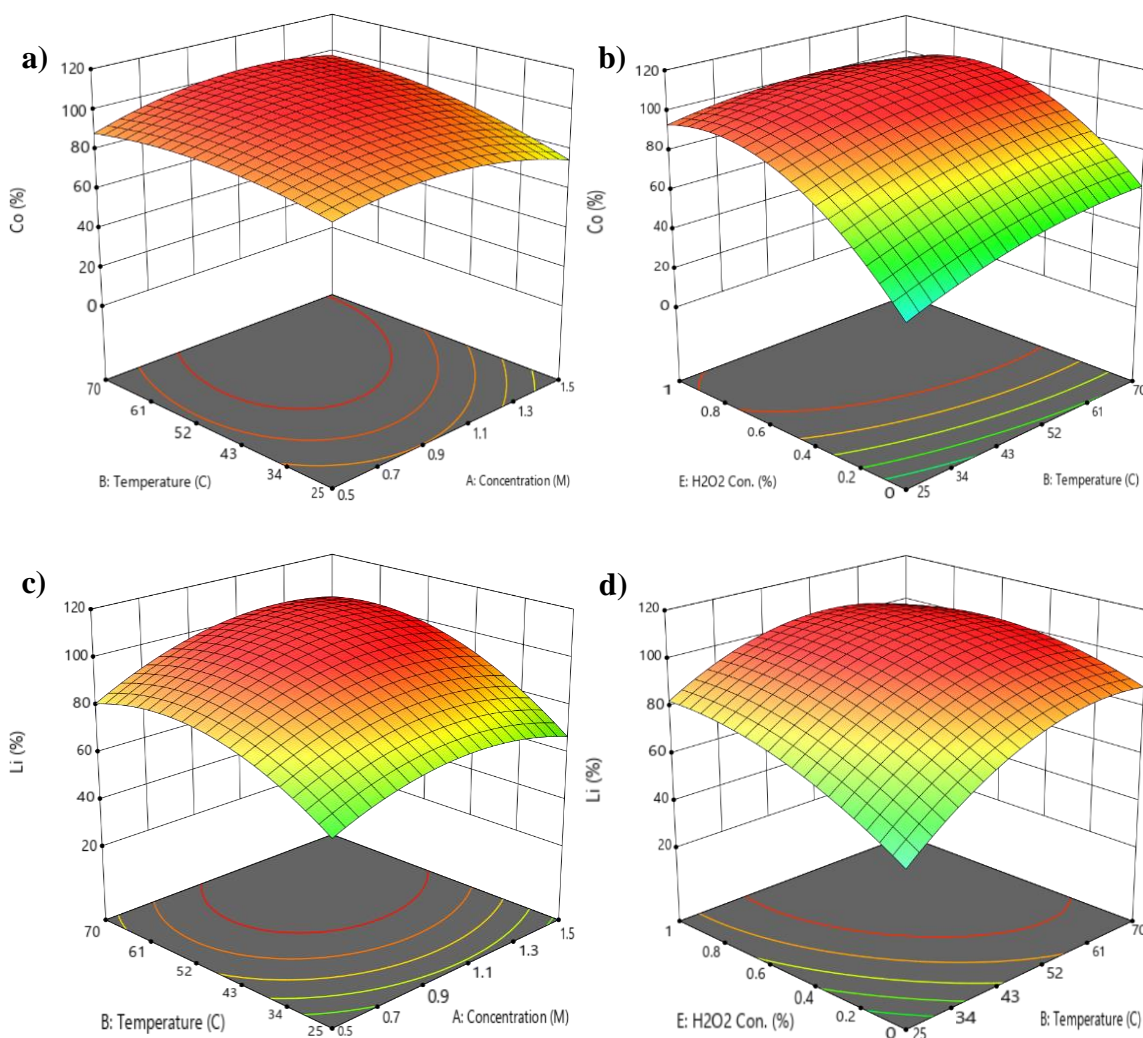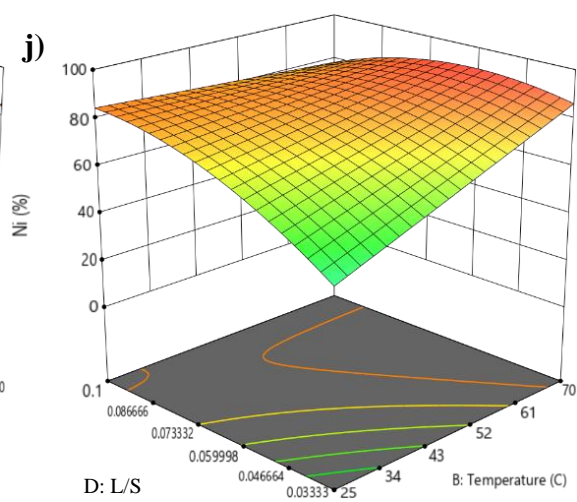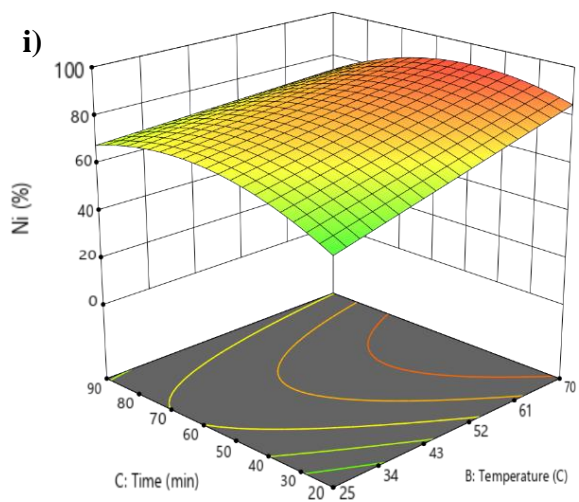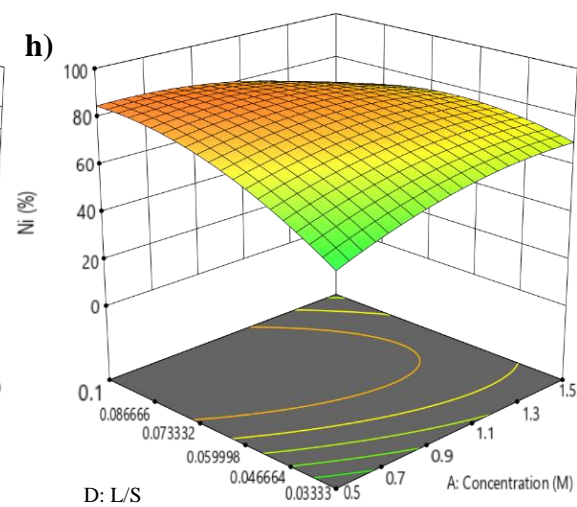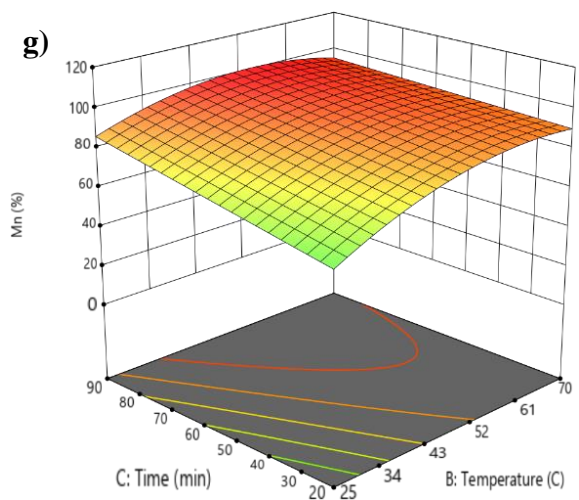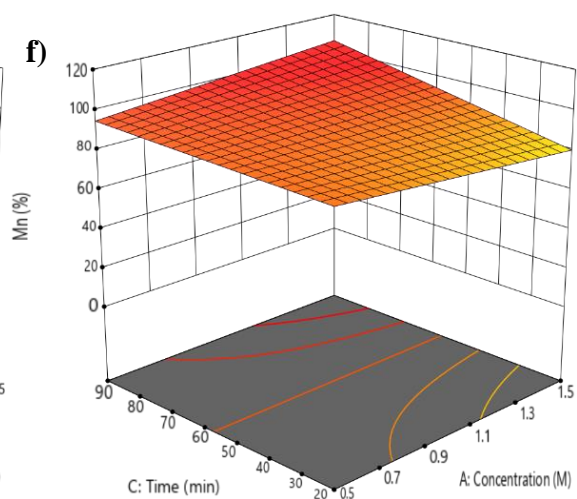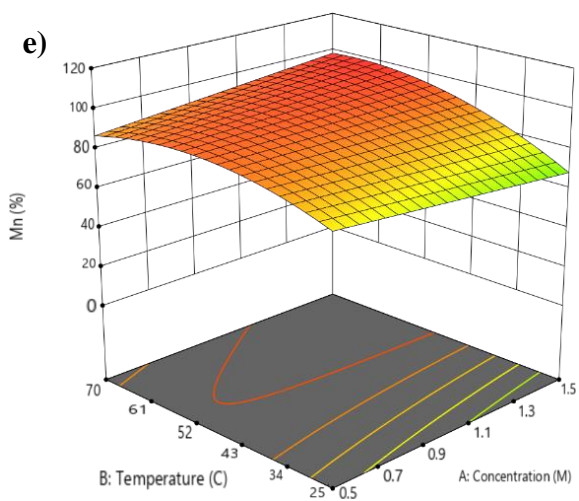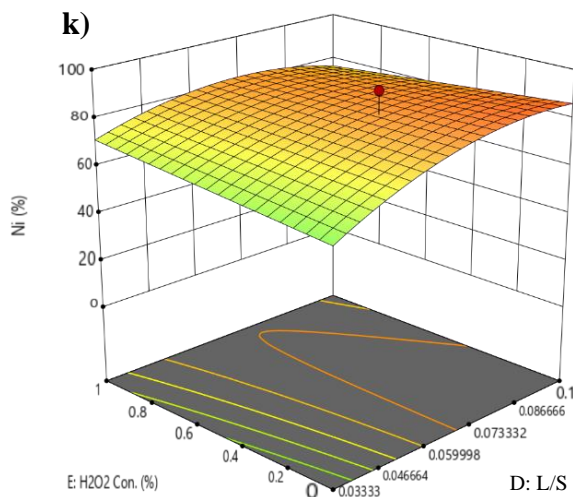
Figure 9. Surface plots for HNO_3. **A)** Co recovery (%) as a function of temperature (ºC) and concentration (M), **b)** Co recovery (%) as a function H_2O_2 conc. (%) and temperature (ºC), **c)** Li recovery (%) as a function of temperature (ºC) and concentration (M), **d)** Li recovery (%) as a function H_2O_2 conc. (%) and temperature (ºC), **e)** Li recovery (%) as a function temperature (ºC) and concentration (M), **f)** Mn recovery (%) as a function of time (min) and concentration (M), **g)** Mn recovery (%) as a function of time (min) and temperature (ºC), **h)** Ni recovery (%) as a function of L/S and concentration (M), **i)** Ni recovery (%) as a function of time (min) and temperature (ºC), **j)** Ni recovery (%) as a function of L/S and temperature (ºC), **k)** Ni recovery (%) as a function H_2O_2 conc. (%) and L/S.

For the RSMs generated for HNO_3, Co recovery (%) is maximum when temperature is higher than 52ºC and the concentration is closer to 1.1 M (Figure 9a), Co recovery (%) is maximum when the H_2O_2 conc. is closer to 0.8% and the temperature is above 52ºC (Figure 9b). Li recovery (%) is maximum when the temperature is between 52 and 61ºC and the concentration is between 1.1 and 1.3 M (Figure 9c), Li recovery (%) is maximum when the H_2O_2 conc. is between 0.6 and 0.8% and the temperature is above 52ºC Figure 9d), Li recovery (%) is maximum when the temperature is closer to 70ºC and the concentration is closer to 1.5 M (Figure 9e). Mn recovery (%) is maximum when the time

(min) and the concentration (M) increase (Figure 9f), Mn recovery (%) is maximum when the time is between 80 and 90 min and the temperature is between 52 and 61℃ (Figure 9g). Ni recovery (%) is maximum when the L/S ratio increases and the concentration is below 0.7 M (Figure 9h), **i** Ni recovery (%) is maximum when the time is between 50 and 60 min and the temperature is closer to 70℃ (Figure 9i), Ni recovery (%) is maximum at two point, one is when the L/S is closer to 0.1 and the temperature is low and the other point is when the L/S ratio is between 0.07 and.0.8 and the temperature is above 60℃ (Figure 9j), Ni recovery (%) is maximum when the H_2O_2 conc. is below 0.4% and the L/S ratio is closer to 0.1 (Figure 9k).

Figure 10 shows that desirability on this model is 0.984 which means that the calculated parameters are 98.4% close to the ideal optimum conditions obtained experimentally in this study.

Desirability = 0.984
Solution 1 out of 86
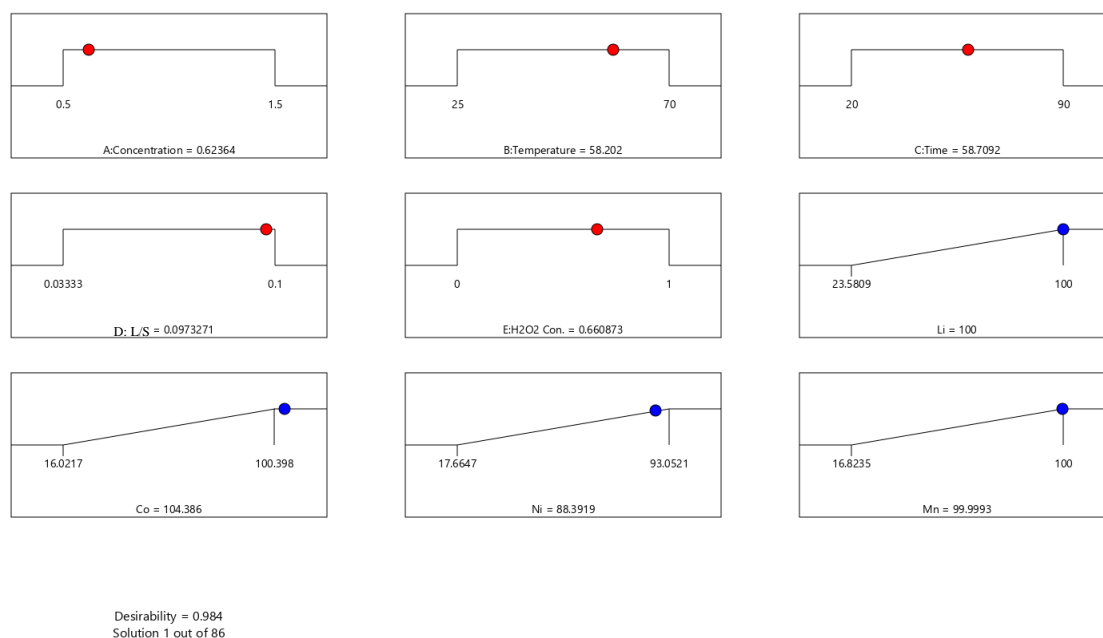
Figure 3. Desirability values of all responses in optimum conditions: 0.62 M, 58.2℃, 58.7min, L/S:0.097 and 0.66 H_2O_2 conc.

3.2.2 Effective Parameters in Leaching

Leaching Agent Nitric acid as a leaching agent has proven that it can also yield high recoveries. When added at 0.62 M and mixed with 0.66% H_2O_2 experimentally it can recover 100% Li, ≈100% Co, 88.3% Ni, and 99.9% Mn.

Temperature At 58.2℃ is the overall lowest temperature of all the inorganic acids studied in this research. For lower temperatures, it was observed that a longer leaching time would be needed as well as higher molarity. At higher temperatures energy would be wasted and inefficient to do at the industrial level.

Time Nitric acid when compared to the leaching time of sulfuric acid and hydrochloric acid, falls in the middle. When in optimal conditions, nitric acid yields high recoveries in 58.7 min.

Overall**,** nitric acid requires less acid and hydrogen peroxide to yield high metal recovery when compared to sulfuric acid and hydrochloric acid. Also, having the lowest temperature among the previously mentioned inorganic acids, makes it energy efficient. On the other hand, having a longer leaching time would have a negative effect on productivity.

3.4 Predicted and validated values

Table 5 shows the predicted response and validated responses for the optimal conditions in for the three inorganic acids used in this study. For H_2SO_4 it can be observed that the predicted responses were lower on the concentration and time but higher on the temperature, L/S ratio and the H_2O_2 conc. but the responses for the recovery of each metal came out to be close between the predicted and validated values. For HCl, the conditions for the predicted and validated values were close to each other, and it can be observed that

the responses were also similar for the metal recovery. Lastly, HNO₃ like the other two

acids show how the predicted and validated values are close to each other as well as the

outcomes of the responses. As previously mentioned, the predicted and validated responses

are close to each other. This validates the statistical design done by the software.

Table 5. A comparison between the predicted and validated results for the optimum conditions for each inorganic acid.

H₂SO₄

Response	Concentration	Temperature	Time	L/S	H_2O_2 Conc.	Li Recovery	Co Recovery	Ni Recovery	Mn Recovery
Predicted	1.96	69.99	20	0.091	0.957	≈100	85.48	96.99	82
Validation 1	2	70	20	0.090	0.813	100	84.5	97	80.5
Validation 2	2	70	20	0.090	0.813	100	84.5	97	80.5

HCl

Response	Concentration	Temperature	Time	L/S	H_2O_2 Conc.	Li Recovery	Co Recovery	Ni Recovery	Mn Recovery
Predicted	1.611	70	90	0.098	0.997	≈100	95.54	100	100
Validation 1	1.6	70	90	0.100	1	98.75	95.69	≈100	≈100
Validation 2	1.6	70	90	0.100	1	98.75	95.69	≈100	≈100

HNO₃

Response	Concentration	Temperature	Time	L/S	H_2O_2 Conc.	Li Recovery	Co Recovery	Ni Recovery	Mn Recovery
Predicted	0.623	58.2	58.71	0.097	0.66	100	≈100	88.39	100
Validation 1	0.6	60	60	0.100	0.65	100	≈100	90	98
Validation 2	0.6	60	60	0.100	0.65	100	≈100	90	98

4.   Life Cycle Assessment

4.1 Methodology

The standard LCA methodology was used which consists in goal and scope, life cycle inventory analysis, life cycle impact assessment and interpretation (Muralikrishna & Manickam, 2017)

4.2 Goal and scope

Under regulations proposed in November 2021, the European Union looks to require that EV batteries contain a minimum of 12% recycled cobalt and 4% recycled lithium and nickel by 2030 (Okinaga, 2021). Therefore, recycling valuable metals used in the lithium-ion battery industry will be in high demand due to the green energy transition happening in the world. For the United States to be able to compete in this market, a clean and efficient way of recycling must be adapted to this industry. This will not only help the economy of the US, but it will also help to contribute to the high demand and scarcity of valuable metals. The primary goal of this research was to evaluate the environmental impacts of the main inorganic acids used in the industry to recycle the valuable metals from NMC 523 powders. This research has proven that hydrochloric acid, nitric acid, and sulfuric acid can dissolve 100% of the Lithium present in the cathode powder. Now it is a matter of demonstrating which acid is less detrimental to the environment through a life cycle assessment.

4.3 Investigated regions

Recycling of lithium-ion batteries is a growing industry that many countries around the world have been working. For this LCA most of the data was collected for the US as

well as the rest of the world to get accurate results. The emissions data for inorganic acids and hydrogen peroxide used rest of the world information. For water and electricity, the emissions from a US standard were collected.

4.4 System boundary and functional unit

This life cycle assessment takes into consideration the consumption of inorganic acid, hydrogen peroxide and water. Industrially, most of the acid and the water used in the process can be recycled and reused. This process generates airborne and waterborne emissions which are also considered in this LCA. The system boundary does not include the dismantling and processing of the powder emissions prior entering the system. Also, solvent extraction and metal production were excluded from this system. In this study, one kilogram of leached lithium processed at a pilot plant was defined as a functional unit. Figure 11 represent a pilot plant that can recover 1 kg of Lithium for each of the inorganic acids and its system boundary.
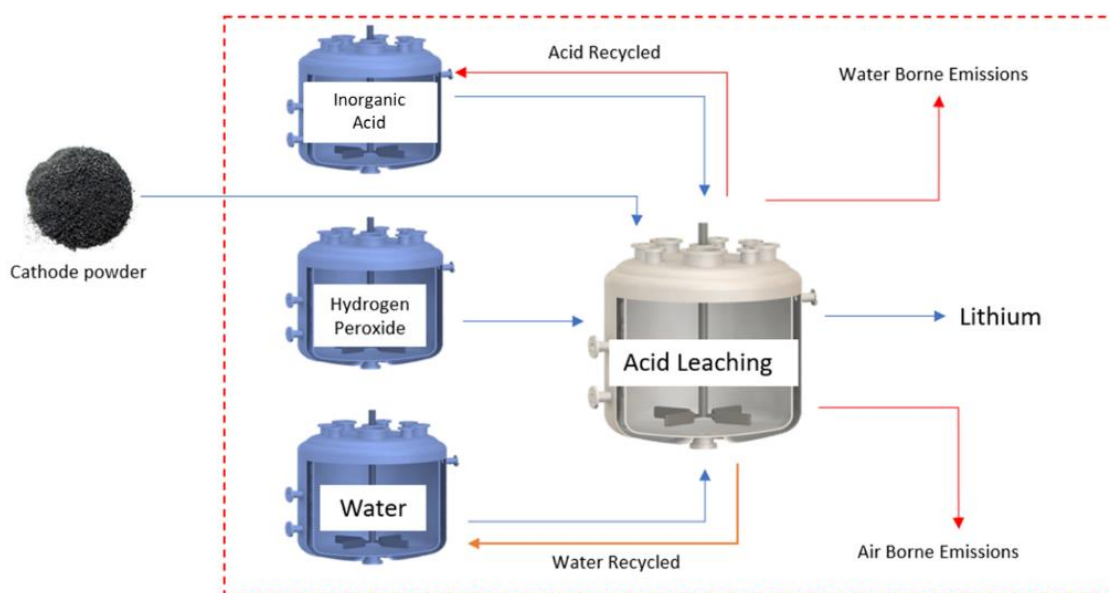
Figure 11. Leaching process using various inorganic acids.

4.5 Life cycle inventory analysis

This research has proven that 100% lithium can be dissolved using HCl, HNO$_3$ and H$_2$SO$_4$ as the main leaching agent. A life cycle assessment was performed to quantify the environmental impacts associated with the critical materials recovery process. Tables 6,7 and 8 show the major material and energy inputs to dissolve 1 kg of Lithium. Data was collected using the LCA software Sima Pro 9 using the TRACI 2.1 V1.04 / US 2008 method and data for the emissions of the boundary previously mentioned. The electricity input comes directly from the heating and stirring of the solution on each of the experiments.

Table 6. Life cycle inventory to obtain 1 kg of Li from the acid leaching stage using HCl.

Inputs/Outputs	Consumption	Unit	UNIT PROCESS
Inputs			
HCl	1.836	Kg	Hydrochloric acid, without water, in 30% solution state {GLO}| tetrafluoroethene production	APOS, U
Water	272.147	Kg	Water, decarbonized {US}| market for water, decarbonized	APOS, U
Electricity	38.57	Kwh	Electricity, medium voltage {US}| market group for	APOS, U
H$_2$O$_2$	0.059	Kg	Hydrogen peroxide, without water, in 50% solution state {RoW}| hydrogen peroxide production, product in 50% solution state	APOS, U
Powder	14.286	kg	Cathode powder from waste/defective NMC LIB batteries
Outputs			
Li	1	kg	Li as Lithium Chloride (LiCl)
Direct Emissions			
Water	12.996	Kg	Wastewater

Table 7. Life cycle inventory to obtain 1 kg of Li from the acid leaching stage using HNO$_3$.

Inputs/Outputs	Consumption	Unit	UNIT PROCESS
Inputs			
HNO$_3$	0.321	Kg	Nitric acid, without water, in 50% solution state {RoW}| nitric acid production, product in 50% solution state	APOS, U
Water	301.84	Kg	Water, decarbonized {US}| market for water, decarbonized	APOS, U
Electricity	25.71	Kwh	Electricity, medium voltage {US}| market group for	APOS, U
H$_2$O$_2$	0.038	Kg	Hydrogen peroxide, without water, in 50% solution state {RoW}| hydrogen peroxide production, product in 50% solution state	APOS, U

Powder	14.286	Kg	Cathode powder from waste/defective NMC LIB batteries
Outputs			
Li	1	Kg	Li as Lithium Nitrate (LiNO3)
Direct Emissions			
Water	14.413	Kg	Waste Water

Table 8. Life cycle inventory to obtain 1 kg of Li from the acid leaching stage using H_2SO_4.

Inputs/Outputs	Consumption	Unit	UNIT PROCESS
Inputs			
H_2SO_4	6.33	Kg	Sulfuric acid {RoW}| production	APOS, U
Water	216.55	Kg	Water, decarbonised {US}| market for water, decarbonised	APOS, U
Electricity	18.856	Kwh	Electricity, medium voltage {US}| market group for	APOS, U
H_2O_2	0.00842	Kg	Hydrogen peroxide, without water, in 50% solution state {RoW}| hydrogen peroxide production, product in 50% solution state	APOS, U
Powder	14.286	Kg	Cathode powder from waste/defective NMC LIB batteries
Outputs			
Li	1	Kg	Li as Lithium Sulfate (LiSO4)
Direct Emissions			
Water	10.959	Kg	Waste Water

To produce one kilogram of lithium, it was found that HCl needed more electricity and hydrogen peroxide when compared to the other inorganic acids. On the other hand, HNO_3, uses the most water out of the three acids. Overall H_2SO_4 uses fewer reagents and resources to recover the same amount of lithium which makes it the most efficient inorganic acid overall. All processes produced waste water that would require further processing.

4.4 Life cycle assessment: baseline

After collecting all the data for the process and getting the values from the LCA software, H_2SO_4 was determined to be the inorganic acid with the lowest environmental impact in the main categories that contribute to the environmental impact out of the three acids used in this research. Hydrochloric acid (HCl) has overall the greater environmental

impact. Even though HNO_3 and H_2SO_4 have bigger impact in a couple categories, HCl is overall the one that causes more harm to the environment. Therefore, Table 9 shows a comparative life cycle assessment using HCl as the baseline for comparison with the other inorganic acids.

Table 9. Comparative Life Cycle impact of producing 1 kg of Li.

Impact category	Unit	HCl	HNO₃	HNO₃/HCl	H₂SO₄	H₂SO₄/HCl
Ozone depletion	kg CFC-11 eq	3.32E-07	2.03E-07	61%	1.26E-07	38%
Global warming	kg CO₂ eq	2.72E+00	2.72E+00	100%	1.25E+00	46%
Smog	kg O₃ eq	9.14E-02	1.02E-01	111%	1.32E-01	145%
Acidification	kg SO₂ eq	5.19E-01	1.17E+00	225%	5.67E-01	109%
Eutrophication	kg N eq	1.79E-02	1.24E-02	69%	8.17E-03	46%
Carcinogenics	CTUh	2.29E-07	1.62E-07	71%	1.46E-07	64%
Non carcinogenics	CTUh	8.13E-07	6.93E-07	85%	8.31E-07	102%
Respiratory effects	kg PM2.5 eq	6.16E-03	4.21E-03	68%	5.29E-03	86%
Ecotoxicity	CTUe	3.47E+01	2.94E+01	85%	6.92E+01	199%
Fossil fuel depletion	MJ surplus	2.51E+00	2.01E+00	80%	4.35E+00	173%

Figure 12 shows the comparison taking the highest impact of each category as 100%. HCl has the highest environmental impact in ozone depletion, global warming, eutrophication, carcinogenics, and respiratory effects making it clearly the worst inorganic acid in this study. HNO_3 has a higher environmental impact in global warming (sharing with HCl) and acidification. Also, it shows above 50% emissions on all other categories but ecotoxicity and fossil fuel depletion which overall performed better than HCl. Lastly, H_2SO_4 has a higher environmental impact in smog, non carcinogenics, ecotoxicity and fossil fuel depletion. On the other categories sulfuric acid has less than 50% emissions but

in carcinogenics and respiratory effects. The remaining four categories which are ozone depletion, global warming, acidification, and eutrophication are below 50% emissions when compared to the other acids which makes H_2SO_4 the acid with the best environmental performance in this study.
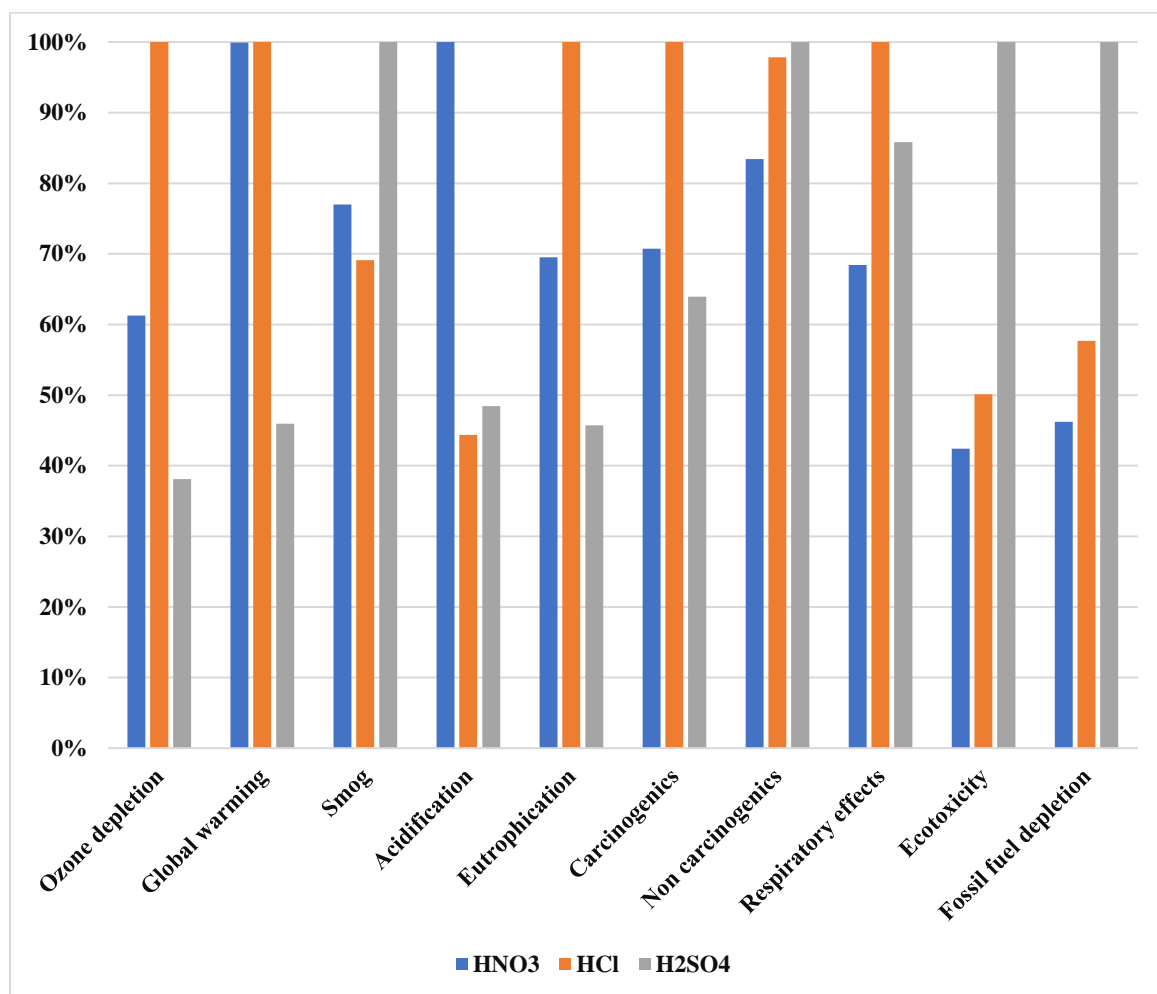
Figure 4. Comparative Life Cycle Impact of Producing 1 kg Li.

Figure 13 shows how each of the components in the leaching process contribute to each category. This shows in detail which component of the process generated most of the impact for each category.

Water as a category plays a minimal role for each of the categories in this study. Only in eutrophication, carcinogenics and non carcinogenics, water can be seen clearly on the graph but again, when compared to the other categories, it only contributes a small percent.

Electricity is the component with the biggest contribution by category. It Is important to point out that the electricity consumption comes from elevating the temperature and the stirring of the solution during the leaching time of each of the optimal conditions for each acid. Because sulfuric acid is the acid with the shortest leaching time and it has required a lower temperature than the other acids, the electricity component is decreased in each category. This means that overall sulfuric acid needs less electricity per category when compared to HCl or HNO_3. Overall hydrochloric has the electricity component as the one with the higher contributor of emissions per category. For nitric acid, the electricity component is balanced with the acid emission for smog and acidification while the remaining categories the electricity is the biggest contributor to the categories' emissions.

Hydrogen peroxide like water, contributions to the emissions per category are almost negligible for each category for all acids.

Acid emissions varies per category but is overall related to the leaching time and temperature for each acid. For HCl and HNO_3 which have a longer leaching time and higher temperatures than sulfuric acid, the acid emissions are lower when compared to the overall emissions of the electricity for every category.
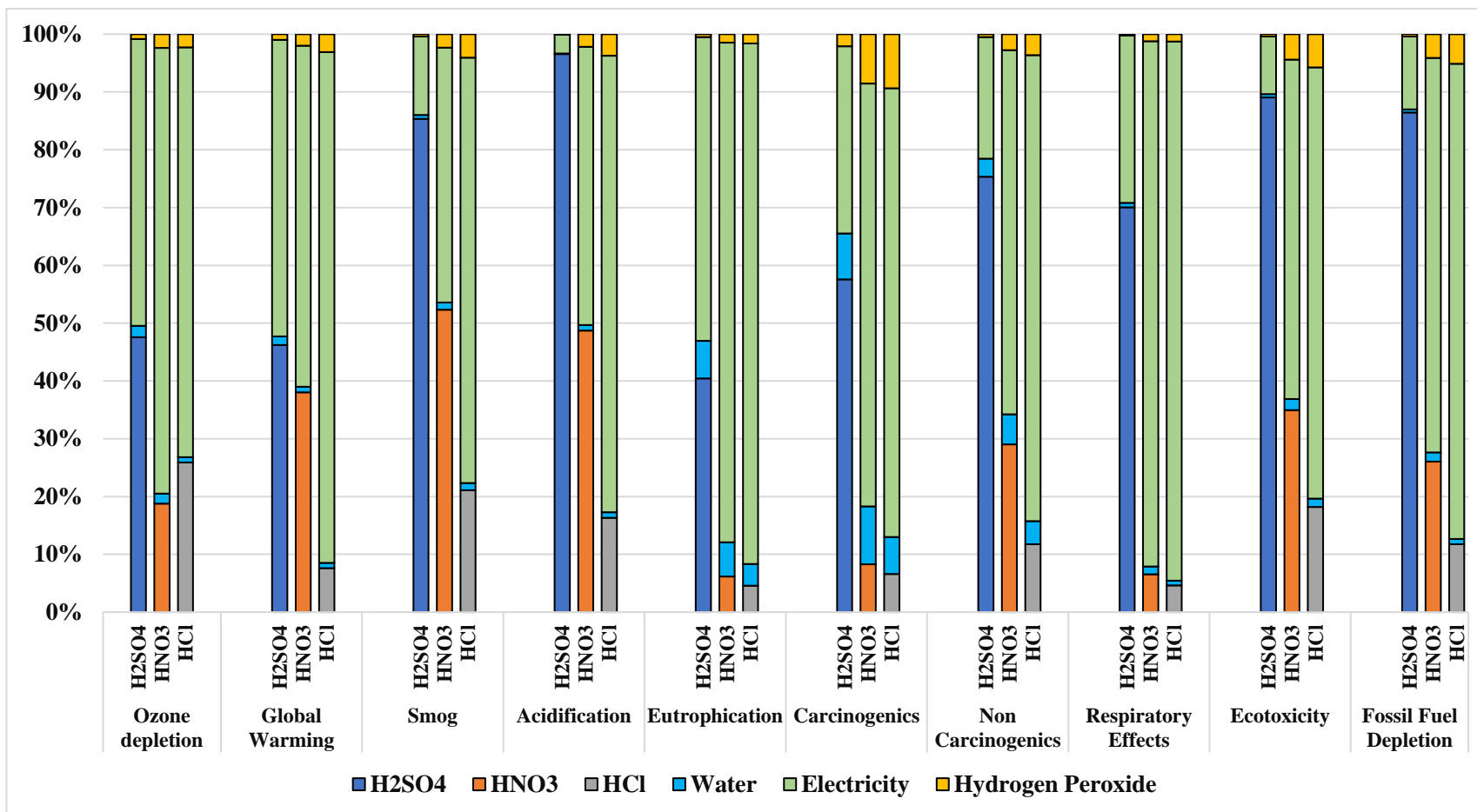
Figure 13. Environmental impacts of each component for different inorganic acids to leach 1 kg of Li.

5.   Co-Additives Effects

After proving that sulfuric acid was the most efficient and environmentally friendly acid. Experiments using sulfuric acid as a primary leaching reagent and glucose and sucrose as co-additives have demonstrated that high metal recoveries can be obtained (X. Chen et al., 2018). The optimal conditions were tested changing the co-additives. This with the purpose to test if other co-additives could match the efficiency of hydrogen peroxide. Sucrose ($C_{12}H_{22}O_{11}$) and glucose ($C_6H_{12}O_6$) were tested with the optimal condition for H_2SO_2 to compare the effects of this organic compounds when compared to hydrogen peroxide. Studies have also tested the combination of different organic co-additives to assist the dissolution of the metals obtaining promising results (Aaltonen et al., 2017)

5.1 Experimental

The parameters for all experiments were 2.5M H_2SO_4, 12.5 (L/S ratio), 24 min and 55 degrees Celsius. For the co-additives, four experiments were performed with H_2O_2, sucrose and glucose. For hydrogen peroxide 0, 0.813, 1.5 and 2% (v/v) was used for each experiment. For glucose and sucrose, 0, 0.2, 0.4 and 0.6 (g/g) was used, were (g/g) meaning that per every gram of cathode powder that amount of co-additive was added. All co-additives were added at the beginning of the experiment and the temperature and stirring was monitored and controlled using a stirring hot plate. And following the same set up as the optimized experiments for H_2SO_4.

5.2 Comparison of organic co-additives

Figure 14 shows the recovery vs the addition of sucrose and glucose per experiment for each element.
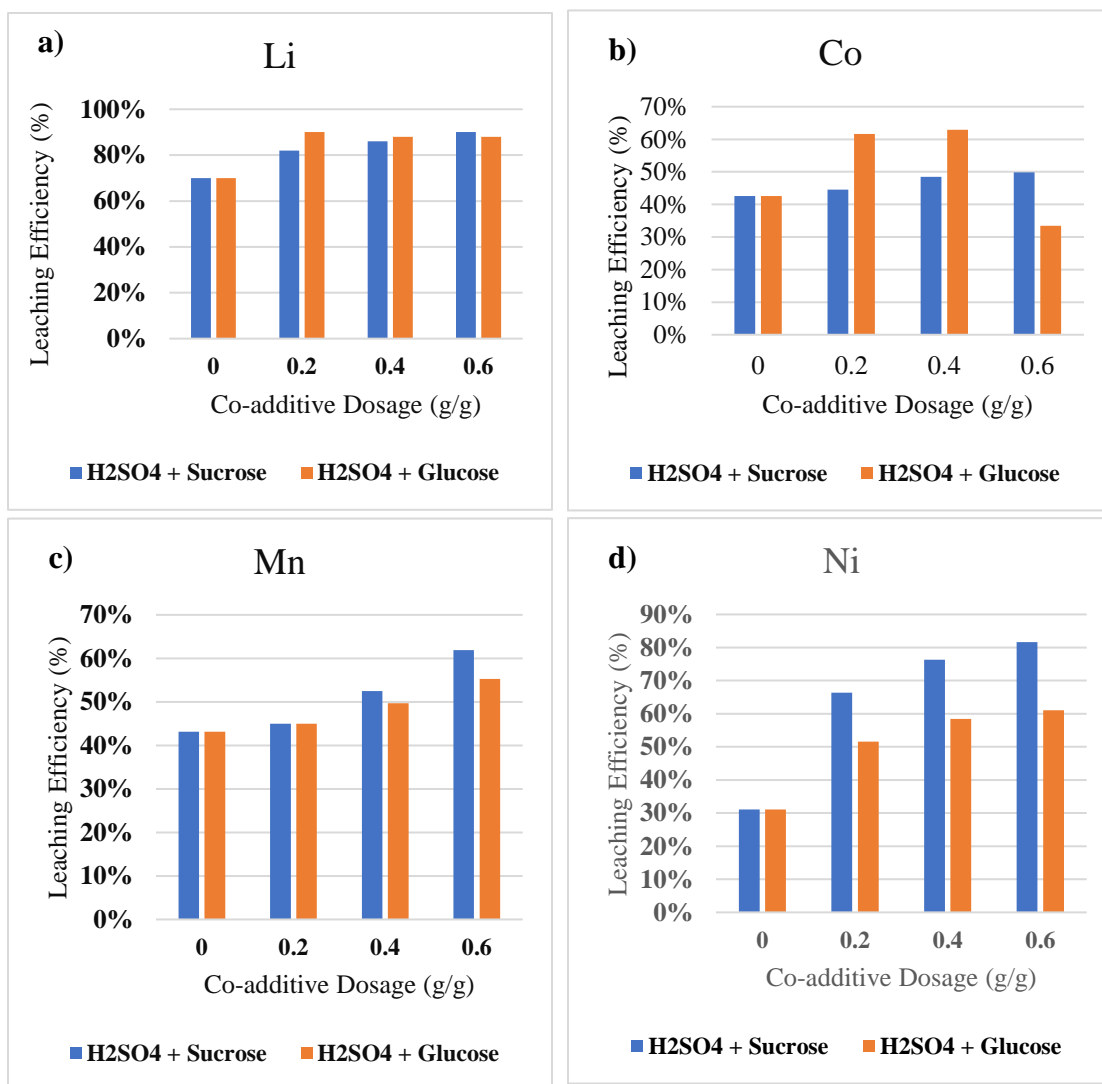
Figure 5. Leaching efficiency vs co-additive dosage for a) lithium, b) cobalt, c) manganese, and d) nickel.

It is important to mention that the conditions used in these experiments were optimized for hydrogen peroxide. Overall, none of these co-additives have the same

recovery as hydrogen peroxide, but it can be concluded that one is more selective than the other. Sucrose seems to increase the recovery of nickel significantly higher than glucose. On the other hand, glucose shows a better overall recovery for cobalt. Lithium and manganese have similar recoveries as the (g/g) for each co-additive increase.

For each experiment the final electric potential (Eh) was measured in millivolts (mV). Figure 15 show the yield (%) vs co-additive addition vs Eh (mv) for H_2O_2, glucose and sucrose.

Figure 15a shows that after 0.8% addition of H_2O_2 and about 385 mv, the recoveries for all four metals do not really improve. So, adding more H_2O_2 will change the Eh but it will be a waste of reagent knowing that the optimal recoveries have been achieved already. The sucrose graph (Figure 15b) shows how as the concentration of sucrose increases, the Eh increases and so do the recoveries for each element. On the other hand, as can be seen in Figure 15c, glucose seems to reach a point were adding more of the co-additive will start slowly decreasing the recoveries. It can be observed that 0.2 (g/g) addition would be the best for this co-additive.
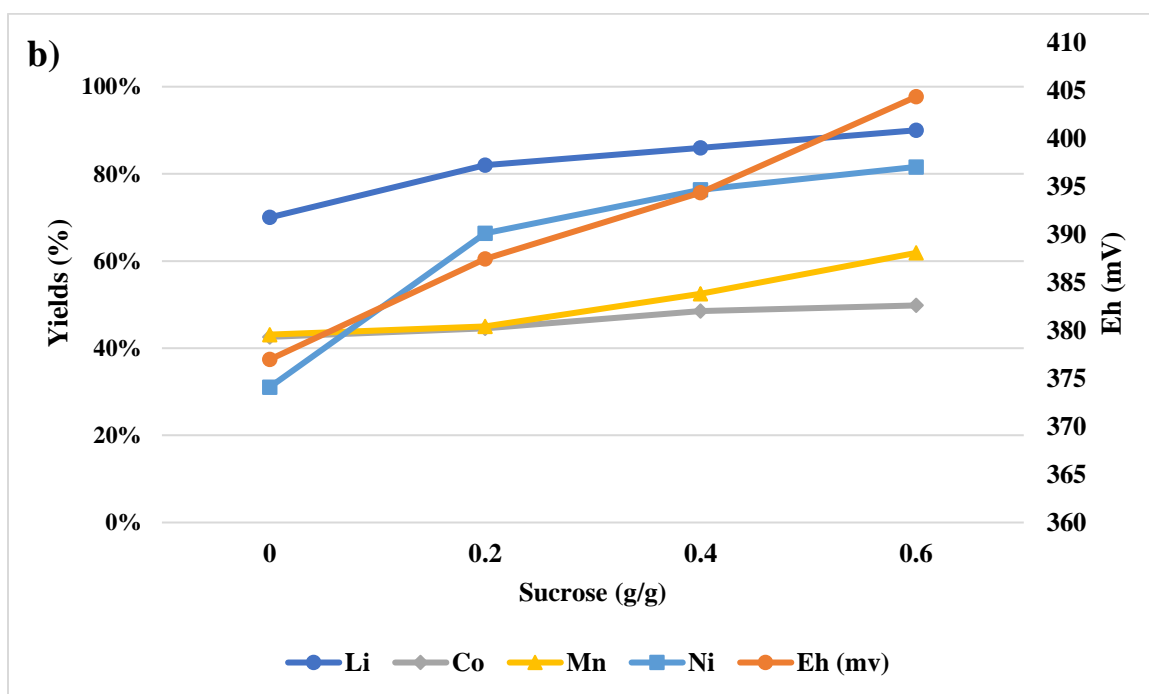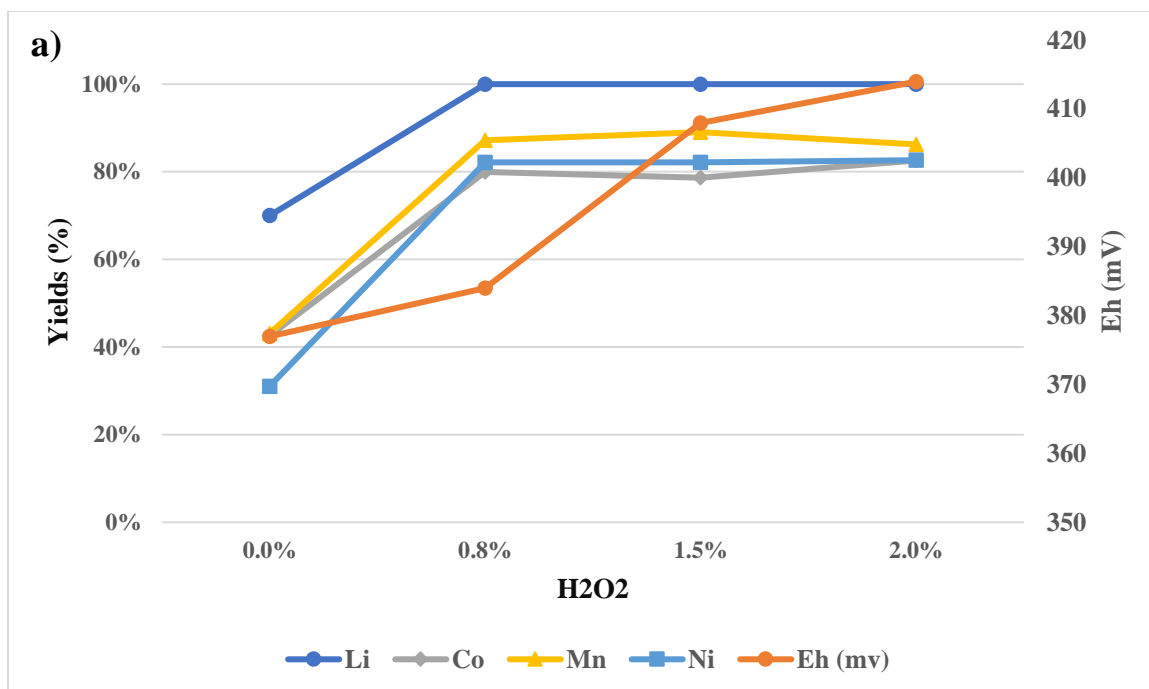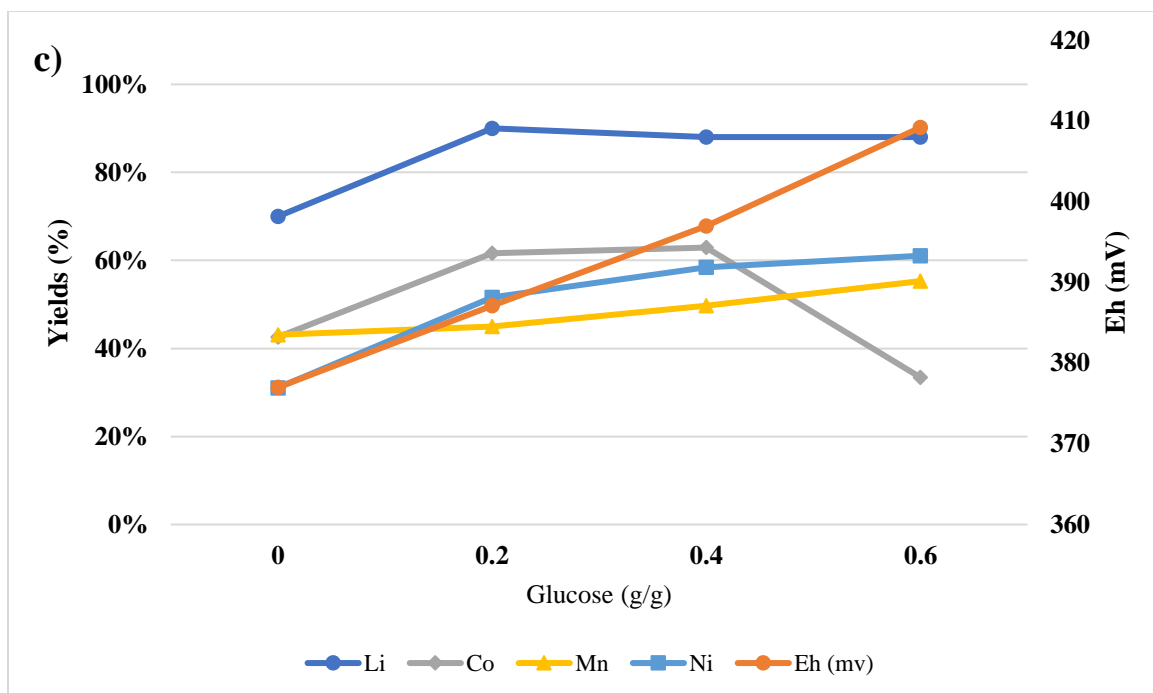
Figure 6. Yield (%) vs co-additive addition vs Eh (mv).

6.   Validation of optimized conditions vs literature

A life cycle assessment was performed to each of the best parameters found in the literature and then they were compared to the results of this study. The parameters from the literature vs the parameters from the optimized conditions of this study are the following:

	Leaching Agent	Concentration M	Temperature (°C)	Time (min)	S/L Ratio (g/l)	H2O2 (vol %)	Efficiency	Year	Source
Literature	H_2SO_4	1	40	60	40	1	Li: 99.7, Ni:99.7, Co:99.7, Mn: 99.7	2017	He et al.
Study	H_2SO_4	2	70	20	0.09	0.813	Li: 100, Ni:97, Co:84.5, Mn: 97		
Literature	HCl	1	90	120	25	20	Li: 94.9, Ni: 94.4, Co: 94.5, Mn: 95.5	2020	Gu et al.
Study	HCl	1.6	70	90	0.1	1	Li: 98.75, Ni: 100, Co: 95.69, Mn: 100		
Literature	HNO_3	1	75	60	20	1.7	Li: 99 Co: 99	2002	Lee & Rhe
Study	HNO_3	0.6	60	60	0.1	0.65	Li: 100, Co: 100, Ni: 90, Mn:100		

Following the same method used for the LCA section in this research, the emissions for the parameters from the literature were calculated. Table 10 shows how the optimized conditions from this study have a better environmental performance in all categories except from acidification. This makes the optimal conditions from this study better than what was previously studied.

Table 10 Comparative LCA H_2SO_4 Study vs Literature

Impact category	Unit	H_2SO_4 Study	H_2SO_4 Literature	H_2SO_4 Study/H_2SO_4 Literature
Ozone depletion	kg CFC-11 eq	3.58E-07	9.28E-07	39%
Global warming	kg CO_2 eq	3.62E+00	9.46E+00	38%
Smog	kg O_3 eq	1.90E-01	3.08E-01	62%

Acidification	kg SO$_2$ eq	5.69E-01	5.60E-01	102%
Eutrophication	kg N eq	2.41E-02	6.36E-02	38%
Carcinogenics	CTUh	3.20E-07	7.36E-07	43%
Non carcinogenics	CTUh	1.44E-06	2.81E-06	51%
Respiratory effects	kg PM2.5 eq	1.07E-02	2.36E-02	46%
Ecotoxicity	CTUe	9.01E+01	1.27E+02	71%
Fossil fuel depletion	MJ surplus	6.10E+00	9.55E+00	64%

Table 11 shows how this study optimized conditions for HCl has a better environmental performance than the literature HCl parameters on all the categories making this study's parameters a better option.

Table 11 Comparative LCA HCl Study vs Literature

Impact category	Unit	HCl Study	HCl Literature	HCl Study/HCl Literature
Ozone depletion	kg CFC-11 eq	3.46E-06	4.56E-06	76%
Global warming	kg CO$_2$ eq	3.47E+01	4.65E+01	74%
Smog	kg O$_3$ eq	9.85E-01	1.32E+00	75%
Acidification	kg SO$_2$ eq	6.10E-01	6.44E-01	95%
Eutrophication	kg N eq	2.32E-01	3.10E-01	75%
Carcinogenics	CTUh	2.59E-06	3.57E-06	73%
Non carcinogenics	CTUh	9.53E-06	1.28E-05	75%
Respiratory effects	kg PM2.5 eq	8.25E-02	1.10E-01	75%
Ecotoxicity	CTUe	3.79E+02	5.11E+02	74%

Fossil fuel depletion	MJ surplus	2.98E+01	4.03E+01	74%

Table 12 shows how this study optimized conditions for HNO_3 has a better environmental performance than the literature HNO_3 conditions on all the categories making this study's parameters a better option.

Table 12 Comparative LCA HNO_3 Study vs Literature

Impact category	Unit	HNO_3 Study	HNO_3 Literature	HNO_3 Study/HNO_3 Literature
Ozone depletion	kg CFC-11 eq	2.29E-06	2.50E-06	91%
Global warming	kg CO_2 eq	2.40E+01	2.61E+01	92%
Smog	kg O_3 eq	6.98E-01	7.52E-01	93%
Acidification	kg SO_2 eq	1.23E+00	1.24E+00	100%
Eutrophication	kg N eq	1.55E-01	1.70E-01	91%
Carcinogenics	CTUh	1.74E-06	1.90E-06	91%
Non carcinogenics	CTUh	6.50E-06	7.08E-06	92%
Respiratory effects	kg PM2.5 eq	5.51E-02	6.05E-02	91%
Ecotoxicity	CTUe	2.59E+02	2.82E+02	92%
Fossil fuel depletion	MJ surplus	2.02E+01	2.21E+01	92%

7.   Conclusions

In this study, the optimal conditions for each leaching agent were found using the design of experiments. The optimal conditions for each acid generated by the software and validated experimentally were:

- H_2SO_4: 1.97 M, 69.99ºC, 20 min, L/S:0.091 and 0.957 H_2O_2 conc.

- HCl: 1.611 M, 69.99ºC, 89.9 min, L/S:0.098 and 0.99 H_2O_2 conc.

- HNO_3: 0.62 M, 58.2ºC, 58.7min, L/S:0.097 and 0.66 H_2O_2 conc.

The optimal conditions found by the design of experiments were validated as the predicted vs validated responses were close to each other for the four metal recoveries. After performing a life cycle assessment for each of the optimal conditions for each acid, sulfuric acid was determined to be the best acid overall. H_2SO_4 has a higher environmental impact in smog, non carcinogenics, ecotoxicity, and fossil fuel depletion. On the ozone depletion, global warming, acidification, and eutrophication categories, sulfuric acid emissions were below 50 % when compared to hydrochloric acid and nitric acid which makes H_2SO_4 the acid with the best environmental performance in this study.

H_2O_2 was the best performing co-additive agent when compared to glucose and sucrose. Even though the other co-additives did not have the same recoveries as hydrogen peroxide, it was found that glucose seems to be more selective when leaching nickel. Similarly, when using sucrose as a co-additive and the optimal conditions for sulfuric acid it was observed that sucrose selectively recovered more cobalt than the glucose.

Overall, all the optimized conditions for each acid had better environmental performance than those conditions found in the literature which validates the optimization of the leaching conditions of this study.

8.   Suggestions for future studies

This study focused on the leaching of NMC 523 powders using inorganic acids. The world is actively seeking more eco-friendly processes for all industries. Therefore, the investigation of leaching other types of NMC powders using organic acids accompanied by a life cycle assessment could eventually probe that organic acid leaching is the future of this industry.

Hydrogen peroxide is the most used co-additive in the industry, but it is hard to produce and difficult to handle. More in-depth analysis should be done to optimize the metal recoveries using other types of co-additives that could match the performance of hydrogen peroxide. As found in this study the selectivity of glucose and sucrose to leach cobalt and nickel respectively could be an area of opportunity if conditions for these co-additives are optimized and look closely. Also, an environmental impact assessment can be performed to the different co-additives and compare them to hydrogen peroxide.

9.   References

Aaltonen, M., Peng, C., Wilson, B. P., & Lundström, M. (2017). Leaching of metals from spent lithium-ion batteries. *Recycling*, *2*(4). https://doi.org/10.3390/recycling2040020

Assefi, M., Maroufi, S., Yamauchi, Y., & Sahajwalla, V. (2020). Pyrometallurgical recycling of Li-ion, Ni–Cd and Ni–MH batteries: A minireview. In *Current Opinion in Green and Sustainable Chemistry* (Vol. 24). https://doi.org/10.1016/j.cogsc.2020.01.005

Aydar, Y. A. (2018). Utilization of Response Surface Methodology in Optimization of Extraction of Plant Materials. *Statistical Approaches With Emphasis on Design of Experiments Applied to Chemical Processes*. https://www.intechopen.com/chapters/59209

Busà, C., Belekoukia, M., & Loveridge, M. J. (2021). The effects of ambient storage conditions on the structural and electrochemical properties of NMC-811 cathodes for Li-ion batteries. *Electrochimica Acta*, *366*. https://doi.org/10.1016/j.electacta.2020.137358

Chen, M., Ma, X., Chen, B., Arsenault, R., Karlson, P., Simon, N., & Wang, Y. (2019). Recycling End-of-Life Electric Vehicle Lithium-Ion Batteries. In *Joule* (Vol. 3, Issue 11). https://doi.org/10.1016/j.joule.2019.09.014

Chen, W. S., & Ho, H. J. (2018). Recovery of valuable metals from lithium-ion batteries NMC cathode waste materials by hydrometallurgical methods. *Metals*, *8*(5).

https://doi.org/10.3390/met8050321

Chen, X., Chen, Y., Zhou, T., Liu, D., Hu, H., & Fan, S. (2015). Hydrometallurgical recovery of metal values from sulfuric acid leaching liquor of spent lithium-ion batteries. *Waste Management*, *38*(1). https://doi.org/10.1016/j.wasman.2014.12.023

Chen, X., Guo, C., Ma, H., Li, J., Zhou, T., Cao, L., & Kang, D. (2018). Organic reductants based leaching : A sustainable process for the recovery of valuable metals from spent lithium ion batteries. *Waste Management*, *75*, 459–468. https://doi.org/10.1016/j.wasman.2018.01.021

Diaz, L. A., Strauss, M. L., Adhikari, B., Klaehn, J. R., McNally, J. S., & Lister, T. E. (2020). Electrochemical-assisted leaching of active materials from lithium ion batteries. *Resources, Conservation and Recycling*, *161*. https://doi.org/10.1016/j.resconrec.2020.104900

Ekberg, C., & Petranikova, M. (2015). Lithium Batteries Recycling. In *Lithium Process Chemistry: Resources, Extraction, Batteries, and Recycling*. https://doi.org/10.1016/B978-0-12-801417-2.00007-4

Gaines, L. (2018). Lithium-ion battery recycling processes: Research towards a sustainable course. *Sustainable Materials and Technologies*, *17*. https://doi.org/10.1016/j.susmat.2018.e00068

Ghassa, S., Farzanegan, A., Gharabaghi, M., & Abdollahi, H. (2020). The reductive leaching of waste lithium ion batteries in presence of iron ions: Process optimization and kinetics modelling. *Journal of Cleaner Production*, *262*.

https://doi.org/10.1016/j.jclepro.2020.121312

Gu, S., Zhang, L., Fu, B., Ahn, J. W., & Wang, X. (2020). Recycling of mixed lithium-
ion battery cathode materials with spent lead-acid battery electrolyte with the
assistance of thermodynamic simulations. *Journal of Cleaner Production*, *266*.
https://doi.org/10.1016/j.jclepro.2020.121827

Guan, J., Li, Y., Guo, Y., Su, R., Gao, G., Song, H., Yuan, H., Liang, B., & Guo, Z.
(2017). Mechanochemical Process Enhanced Cobalt and Lithium Recycling from
Wasted Lithium-Ion Batteries. *ACS Sustainable Chemistry and Engineering*, *5*(1),
1026–1032. https://doi.org/10.1021/acssuschemeng.6b02337

Guo, Y., Li, F., Zhu, H., Li, G., Huang, J., & He, W. (2016). Leaching lithium from the
anode electrode materials of spent lithium-ion batteries by hydrochloric acid (HCl).
Waste Management, *51*. https://doi.org/10.1016/j.wasman.2015.11.036

He, L. P., Sun, S. Y., Song, X. F., & Yu, J. G. (2017). Leaching process for recovering
valuable metals from the LiNi1/3Co1/3Mn1/3O2 cathode of lithium-ion batteries.
Waste Management, *64*. https://doi.org/10.1016/j.wasman.2017.02.011

He, L. P., Sun, S. Y., & Yu, J. G. (2018). Performance of LiNi1/3Co1/3Mn1/3O2
prepared from spent lithium-ion batteries by a carbonate co-precipitation method.
Ceramics International, *44*(1). https://doi.org/10.1016/j.ceramint.2017.09.180

IEA. (2020). *Global EV Outlook 2020*. Technology Report.
https://www.iea.org/reports/global-ev-outlook-2020

Jehle, C. (2021). *NMC, LFP, LTO. What's the Difference? [The Battery Cycle #2]*. The

Battery Cycle. https://www.sustainable-bus.com/news/nmc-lfp-lto-battery-explained/

Jiang, J. J., & Zeng, X. L. (2015). Feasibility Analysis of Recycling and Disposal of Spent Lithium-Ion Batteries in China. *Applied Mechanics and Materials*, *768*, 622–626. https://www.scientific.net/AMM.768.622

Jones, B., Elliott, R. J. R., & Nguyen-Tien, V. (2020). The EV revolution: The road ahead for critical raw materials demand. *Applied Energy*, *280*. https://doi.org/10.1016/j.apenergy.2020.115072

Kane, M. (2019). *91% Of Lithium For Lithium-Ion Batteries Comes From Three Countries*. Battery Tech. https://insideevs.com/news/372133/91-of-lithium-three-countries/

Lee, C. K., & Rhee, K. I. (2002). Preparation of LiCoO2 from spent lithium-ion batteries. *Journal of Power Sources*, *109*(1). https://doi.org/10.1016/S0378-7753(02)00037-X

Lin, L. (2020). Recovery of valuable metals fr aluable metals from spent lithium-ion batteries om spent lithium-ion batteries using organic acids: assessment of technoeconomic feasibility. *Public Health*, 125. http://scholar.google.com/scholar?hl=en&btnG=Search&q=intitle:Some+Contributions+on+MIMO+Radar#0

Meshram, P., Abhilash, Pandey, B. D., Mankhand, T. R., & Deveci, H. (2016). Comparision of Different Reductants in Leaching of Spent Lithium Ion Batteries. *JOM*, *68*(10). https://doi.org/10.1007/s11837-016-2032-9

Meshram, P., Mishra, A., Abhilash, & Sahu, R. (2020). Environmental impact of spent
lithium ion batteries and green recycling perspectives by organic acids – A review.
In *Chemosphere* (Vol. 242). https://doi.org/10.1016/j.chemosphere.2019.125291

Muralikrishna, I. V., & Manickam, V. (2017). Life Cycle Assessment. *Environmental
Management*, 57–75. https://doi.org/10.1016/B978-0-12-811989-1.00005-1

Muzayanha, S. U., Yudha, C. S., Nur, A., Widiyandari, H., Haerudin, H., Nilasary, H.,
Fathoni, F., & Purwanto, A. (2019). A fast metals recovery method for the synthesis
of lithium nickel cobalt aluminum oxide material from cathode waste. *Metals*, *9*(5).
https://doi.org/10.3390/met9050615

Nickel Institute. (2020). *Nickel is making a vital contribution to the lithium-ion (Li-ion)
batteries that power much of the electric vehicle revolution.*
https://nickelinstitute.org/about-nickel/nickel-in-batteries/

Nitta, N., Wu, F., Lee, J. T., & Yushin, G. (2015). Li-ion battery materials: Present and
future. In *Materials Today* (Vol. 18, Issue 5).
https://doi.org/10.1016/j.mattod.2014.10.040

Nshizirungu, T., Agarwal, A., Jo, Y. T., Rana, M., Shin, D., & Park, J. H. (2020).
Chlorinated polyvinyl chloride (CPVC) assisted leaching of lithium and cobalt from
spent lithium-ion battery in subcritical water. *Journal of Hazardous Materials*, *393*.
https://doi.org/10.1016/j.jhazmat.2020.122367

Okinaga, S. (2021). *EV batteries: Cheaper way to recycle material developed in Japan*.
https://asia.nikkei.com/Business/Markets/Commodities/EV-batteries-Cheaper-way-

to-recycle-material-developed-in-Japan

Or, T. et. al. (2019). *Recycling of mixed cathode lithium-ion batteries for electric vehicles_ Current status and future outlook _ Enhanced Reader.pdf*. Carbon Energy Wiley.

Ore, I., Pigments, I. O., Rock, P., Crystal, Q., Earths, R., & Ash, S. (2021). *MINERAL COMMODITY SUMMARIES 2021*.

Sarabia, L. A., & Ortiz, M. C. (2009). Response Surface Methodology. *Comprehensive Chemometrics*, *1*, 345–390. https://doi.org/10.1016/B978-044452701-1.00083-1

Stan, A. I., Swierczynski, M., Stroe, D. I., Teodorescu, R., & Andreasen, S. J. (2014). Lithium ion battery chemistries from renewable energy storage to automotive and back-up power applications - An overview. *2014 International Conference on Optimization of Electrical and Electronic Equipment, OPTIM 2014*, 713–720. https://doi.org/10.1109/OPTIM.2014.6850936

Tabelin, C. B., Dallas, J., Casanova, S., Pelech, T., Bournival, G., Saydam, S., & Canbulat, I. (2021). Towards a low-carbon society: A review of lithium resource availability, challenges and innovations in mining, extraction and recycling, and future perspectives. In *Minerals Engineering* (Vol. 163). https://doi.org/10.1016/j.mineng.2020.106743

Urbańska, W. (2020). Recovery of Co, Li, and Ni from spent li-ion batteries by the inorganic and/or organic reducer assisted leaching method. *Minerals*, *10*(6), 1–13. https://doi.org/10.3390/min10060555

USDOE. (2020). *Department of Energy (DOE) Office of Energy Efficiency and Renewable Energy (EERE) FY2020 AMO Critical Materials FOA : Next - Generation Technologies and Field Validation*.

USGS. (2018). *Mineral Commodity Summaries 2018*.

USGS. (2020). *DE-FOA-0002358 : Request for Information on the Office of Energy Efficiency & Renewable Energy ' s in support of Battery Critical Materials Supply Chain R & D*.

Wang, B. (n.d.). *World Battery Production*. Energy and Sustainability Network. https://energycentral.com/c/ec/world-battery-production

Wu, S., Tao, W., Zheng, Y., Ge, H., He, J., Yang, Y., & Wang, Z. (2021). A novel approach for lithium recovery from waste lithium-containing aluminum electrolyte by a roasting-leaching process. *Waste Management*, *134*. https://doi.org/10.1016/j.wasman.2021.08.011

Xu, C., Dai, Q., Gaines, L., Hu, M., Tukker, A., & Steubing, B. (2020). Future material demand for automotive lithium-based batteries. *Communications Materials*, *1*(1). https://doi.org/10.1038/s43246-020-00095-x

Xuan, W., Otsuki, A., & Chagnes, A. (2019). Investigation of the leaching mechanism of NMC 811 (LiNi0.8Mn0.1Co0.1O2) by hydrochloric acid for recycling lithium ion battery cathodes. *RSC Advances*, *9*(66), 38612–38618. https://doi.org/10.1039/c9ra06686a

Yabuuchi, N., & Ohzuku, T. (2003). Novel lithium insertion material of

LiCo1/3Ni1/3Mn1/3O2 for advanced lithium-ion batteries. *Journal of Power Sources*, *119–121*. https://doi.org/10.1016/S0378-7753(03)00173-3

Yang, J., JIANG, L. xing, LIU, F. yang, JIA, M., & LAI, Y. qing. (2020). Reductive acid leaching of valuable metals from spent lithium-ion batteries using hydrazine sulfate as reductant. *Transactions of Nonferrous Metals Society of China (English Edition)*, *30*(8). https://doi.org/10.1016/S1003-6326(20)65376-6

Zhang, G., Du, Z., He, Y., Wang, H., Xie, W., & Zhang, T. (2019). A sustainable process for the recovery of anode and cathode materials derived from spent lithium-ion batteries. *Sustainability (Switzerland)*, *11*(8). https://doi.org/10.3390/su11082363

10. Appendix

10. 0 Leaching equations

The main reactions in the leaching process for the three main acids used in this study are as follows:

HCl:

$$2LiMO_{2(s)} + 8HCl_{(l)} \rightleftharpoons 2LiCl_{(l)} + 2MCl2_{(l)} + 4H_2O_{(l)} + Cl_{2(g)} \ldots(\text{Xuan et al., 2019}) \qquad (1)$$

H_2SO_4:

$$6LiNi_{1/3}Mn_{1/3}Co_{1/3}O_{2(s)} + 9H_2SO_{4(aq)} + H_2O_{2(aq)} \rightleftharpoons 2MnSO_{4(aq)} + 2NiSO_{4(aq)} + 2CoSO_{4(aq)} + 3Li_2SO_{4(aq)}$$
$$+ 10H_2O_{(g)} + 2O_{2(g)} \ldots(\text{W. S. Chen \& Ho, 2018}) \qquad (2)$$

HNO_3:
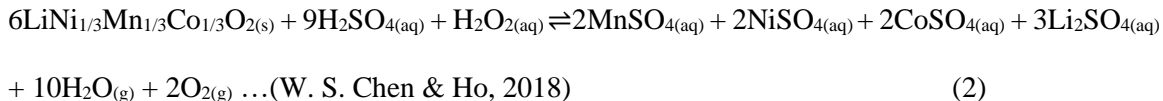
$$3HNO_{3(aq)} + LiMO_2 \rightleftharpoons LiNO_3(aq) + 0.8Ni(NO3)_{2(aq)} + 0.15Co(NO_3)_2(aq) +$$
$$0.05Al(NO_3)_{2(aq)} + 1.5H_2O_{(liq)} + 0.5O_{2(g)} \ldots (\text{Muzayanha et al., 2019}) \qquad (3)$$
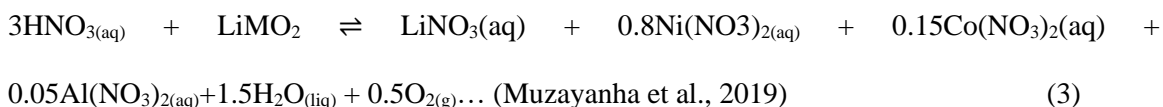
From these equations, it can be seen how the main acid dissociates as H^+ and Cl^-, SO_4^{2-} and NO_3^- respectively. The hydrogen proton forms H_2O while the metal bonds with the anion and O_2 is produced in all the reactions.

10.1 ANOVA tables and Statistics for H_2SO_4

ANOVA for Reduced Quadratic model

Response 1: Li

Source	Sum of Squares	df	Mean Square	F-value	p-value	
Model	8132.52	15	542.17	9.97	< 0.0001	significant

A-Concentration	1773.39	1 1773.39	32.62	< 0.0001
B-Temperature	1093.96	1 1093.96	20.13	0.0006
C-Time	553.28	1 553.28	10.18	0.0071
D-L/S	336.05	1 336.05	6.18	0.0273
E-H2O2 Con.	543.03	1 543.03	9.99	0.0075
AB	264.06	1 264.06	4.86	0.0462
AC	232.56	1 232.56	4.28	0.0591
BC	370.56	1 370.56	6.82	0.0216
BD	115.56	1 115.56	2.13	0.1686
BE	138.06	1 138.06	2.54	0.1350
DE	217.56	1 217.56	4.00	0.0668
A²	330.30	1 330.30	6.08	0.0284
B²	466.01	1 466.01	8.57	0.0118
C²	101.79	1 101.79	1.87	0.1944
E²	181.50	1 181.50	3.34	0.0907
Residual	706.65	13 54.36		
Lack of Fit	692.65	10 69.26	14.84	0.0240 significant
Pure Error	14.00	3 4.67		
Cor Total	8839.17	28		

Fit Statistics

Std. Dev. 7.37	**R²**	0.9201
Mean 82.55	**Adjusted R²**	0.8278
C.V. % 8.93	**Predicted R²**	0.4244
	Adeq Precision 12.5962	

Final Equation in Terms of Coded Factors

Co   =

+74.69

+6.71   A

+5.33   B

+5.10   C

+21.28 E

-5.06   AB

-4.69   AC

+3.81   AE

-2.06   BC

-3.19   BD

+4.19   BE

+2.81   CE

-3.27   A²

-3.38   B²

-2.66   C²

-16.59 E²

ANOVA for Reduced Quadratic model

Response 2: Co

Source	Sum of Squares	df	Mean Square	F-value	p-value	
Model	15088.79	15	1005.92	18.87	< 0.0001	significant
A-Concentration	747.05	1	747.05	14.01	0.0025	

B-Temperature	580.97	1	580.97	10.90	0.0057
C-Time	532.70	1	532.70	9.99	0.0075
E-H2O2 Con.	8395.46	1	8395.46	157.47	< 0.0001
AB	410.06	1	410.06	7.69	0.0158
AC	351.56	1	351.56	6.59	0.0234
AE	232.56	1	232.56	4.36	0.0570
BC	68.06	1	68.06	1.28	0.2789
BD	162.56	1	162.56	3.05	0.1043
BE	280.56	1	280.56	5.26	0.0391
CE	126.56	1	126.56	2.37	0.1474
A²	70.54	1	70.54	1.32	0.2708
B²	115.11	1	115.11	2.16	0.1655
C²	72.90	1	72.90	1.37	0.2632
E²	1944.70	1	1944.70	36.48	< 0.0001
Residual	693.07	13	53.31		
Lack of Fit	507.07	10	50.71	0.8179	0.6483	not significant
Pure Error	186.00	3	62.00		
Cor Total	15781.86	28			

Fit Statistics

Std. Dev.	7.30	**R²**		0.9561
Mean	58.07	**Adjusted R²**		0.9054
C.V. %	12.57	**Predicted R²**		0.7364
		Adeq Precision		13.8817

Final Equation in Terms of Coded Factors

Co   =

+74.69

+6.71 A

+5.33 B

+5.10 C

+21.28 E

-5.06 AB

-4.69 AC

+3.81 AE

-2.06 BC

-3.19 BD

+4.19 BE

+2.81 CE

-3.27 A²

-3.38 B²

-2.66 C²

-16.59 E²

ANOVA for Reduced Quadratic model

Response 3: Mn

Source	Sum of Squares	df	Mean Square	F-value	p-value	
Model	10553.20	13	811.78	12.40	< 0.0001	significant
A-Concentration	616.49	1	616.49	9.42	0.0078	
B-Temperature	371.18	1	371.18	5.67	0.0309	
D-L/S	365.29	1	365.29	5.58	0.0321	
E-H2O2 Con.	3922.81	1	3922.81	59.92	< 0.0001	
AB	175.56	1	175.56	2.68	0.1223	

AC	68.06	1	68.06	1.04	0.3241
BC	770.06	1	770.06	11.76	0.0037
BD	105.06	1	105.06	1.60	0.2245
BE	68.06	1	68.06	1.04	0.3241
CD	95.06	1	95.06	1.45	0.2469
B²	612.77	1	612.77	9.36	0.0079
D²	148.58	1	148.58	2.27	0.1527
E²	2262.33	1	2262.33	34.56	< 0.0001
Residual	981.98	15	65.47		
Lack of Fit	697.23	12	58.10	0.6121	0.7663 not significant
Pure Error	284.75	3	94.92		
Cor Total	11535.17	28			

Fit Statistics

Std. Dev.	8.09	**R²**	0.9149
Mean	47.55	**Adjusted R²**	0.8411
C.V. %	17.02	**Predicted R²**	0.7153
		Adeq Precision	12.0164

Final Equation in Terms of Coded Factors

Mn   =

+66.05

+5.86 A

+4.26 B

+4.22 D

+14.50 E

-3.31 AB

-2.06   AC

-6.94   BC

+2.56   BD

+2.06   BE

-2.44   CD

-7.59   B²

-3.71   D²

-16.69 E²

ANOVA for Reduced Quadratic model

Response 4: Ni

Source	Sum of Squares	df	Mean Square	F-value	p-value	
Model	17154.44	16	1072.15	23.07	< 0.0001	significant
B-Temperature	370.99	1	370.99	7.98	0.0153	
C-Time	935.72	1	935.72	20.13	0.0007	
D-L/S	1032.98	1	1032.98	22.23	0.0005	
E-H2O2 Con.	5840.15	1	5840.15	125.66	< 0.0001	
AB	1190.25	1	1190.25	25.61	0.0003	
AC	1225.00	1	1225.00	26.36	0.0002	
AD	240.25	1	240.25	5.17	0.0422	
AE	240.25	1	240.25	5.17	0.0422	
BD	100.00	1	100.00	2.15	0.1681	
BE	121.00	1	121.00	2.60	0.1326	
CD	156.25	1	156.25	3.36	0.0916	
CE	210.25	1	210.25	4.52	0.0549	
A²	150.07	1	150.07	3.23	0.0975	

B²	635.32	1	635.32	13.67	0.0031	
D²	595.46	1	595.46	12.81	0.0038	
E²	1730.43	1	1730.43	37.23	< 0.0001	
Residual	557.70	12	46.48			
Lack of Fit	544.95	9	60.55	14.25	0.0256	significant
Pure Error	12.75	3	4.25			
Cor Total	17712.14	28				

Fit Statistics

Std. Dev.	6.82	**R²**	0.9685
Mean	70.83	**Adjusted R²**	0.9265
C.V. %	9.63	**Predicted R²**	0.7269
		Adeq Precision	16.0877

Final Equation in Terms of Coded Factors

Ni   =

+94.61

+4.26 B

+6.76 C

+7.10 D

+17.74 E

-8.62 AB

-8.75 AC

-3.87 AD

+3.87 AE

-2.50 BD

-2.75 BE

+3.13 CD

-3.63 CE

-4.58 A²

-7.89 B²

-7.59 D²

-15.49 E²

10.2 ANOVA tables and Statistics for HCl

ANOVA for Reduced Quadratic model
Response 1: Li

Source	Sum of Squares	df	Mean Square	F-value	p-value	
Model	9351.11	12	779.26	13.35	< 0.0001	significant
A-Concentration	2282.59	1	2282.59	39.11	< 0.0001	
B-Temperature	770.57	1	770.57	13.20	0.0021	
C-Time	295.03	1	295.03	5.05	0.0381	
D-L/S	1554.34	1	1554.34	26.63	< 0.0001	
E-H2O2 Con.	429.04	1	429.04	7.35	0.0148	
AC	169.00	1	169.00	2.90	0.1070	
AD	342.25	1	342.25	5.86	0.0269	
BC	256.00	1	256.00	4.39	0.0515	
BE	306.25	1	306.25	5.25	0.0350	
DE	240.25	1	240.25	4.12	0.0584	
A²	2013.91	1	2013.91	34.50	< 0.0001	
D²	249.09	1	249.09	4.27	0.0544	
Residual	992.26	17	58.37			

Source	Sum of Squares	df	Mean Square	F-value	p-value	
Lack of Fit	979.51	14	69.96	16.46	0.0204	significant
Pure Error	12.75	3	4.25			
Cor Total	10343.37	29				

ANOVA for Reduced Quadratic model

Response 2: Co

Source	Sum of Squares	df	Mean Square	F-value	p-value	
Model	17442.31	11	1585.66	8.50	< 0.0001	significant
A-Concentration	4124.82	1	4124.82	22.12	0.0002	
B-Temperature	343.17	1	343.17	1.84	0.1917	
D-L/S	1740.98	1	1740.98	9.33	0.0068	
E-H2O2 Con.	5250.10	1	5250.10	28.15	< 0.0001	
AD	992.25	1	992.25	5.32	0.0332	
BC	506.25	1	506.25	2.71	0.1168	
BE	1089.00	1	1089.00	5.84	0.0265	
CD	380.25	1	380.25	2.04	0.1704	
DE	1089.00	1	1089.00	5.84	0.0265	
A²	1184.67	1	1184.67	6.35	0.0214	
E²	486.79	1	486.79	2.61	0.1236	
Residual	3357.06	18	186.50			
Lack of Fit	2234.31	15	148.95	0.3980	0.9020	not significant
Pure Error	1122.75	3	374.25			
Cor Total	20799.37	29				

Fit Statistics

Std. Dev. 13.66	**R²**	0.8386	
Mean 71.57	**Adjusted R²**	0.7400	

C.V. % 19.08 **Predicted R²** 0.5850

Adeq Precision 9.9036

Final Equation in Terms of Coded Factors

Co =

+82.78

+14.20 A

+4.17 B

+9.22 D

+16.73 E

-7.87 AD

-5.62 BC

-8.25 BE

-4.87 CD

+8.25 DE

-10.25 A²

-7.04 E²

ANOVA for Reduced Quadratic model

Response 3: Ni

Source	Sum of Squares	df	Mean Square	F-value	p-value	
Model	23916.32	14	1708.31	12.12	< 0.0001	significant
A-Concentration	6010.55	1	6010.55	42.65	< 0.0001	
B-Temperature	2017.50	1	2017.50	14.32	0.0018	
D-L/S	2295.06	1	2295.06	16.29	0.0011	
E-H2O2 Con.	1221.91	1	1221.91	8.67	0.0100	
AC	1072.56	1	1072.56	7.61	0.0146	

AD	1785.06	1	1785.06	12.67	0.0029	
AE	1350.56	1	1350.56	9.58	0.0074	
BD	3751.56	1	3751.56	26.62	0.0001	
CD	264.06	1	264.06	1.87	0.1912	
CE	430.56	1	430.56	3.06	0.1009	
A²	1728.06	1	1728.06	12.26	0.0032	
B²	567.33	1	567.33	4.03	0.0632	
D²	797.98	1	797.98	5.66	0.0310	
E²	284.31	1	284.31	2.02	0.1759	
Residual	2113.68	15	140.91			
Lack of Fit	1535.68	12	127.97	0.6642	0.7368	not significant
Pure Error	578.00	3	192.67			
Cor Total	26030.00	29				

Fit Statistics

Std. Dev.	11.87	**R²**	0.9188
Mean	57.00	**Adjusted R²**	0.8430
C.V. %	20.83	**Predicted R²**	0.7710
		Adeq Precision	12.1863

Final Equation in Terms of Coded Factors

Ni   =

+62.17

+17.14 A

+10.18 B

-10.59 D

+8.11 E

+8.19 AC

-10.56 AD

-9.19 AE

+15.31 BD

+4.06 CD

+5.19 CE

-12.62 A²

+8.10 B²

-8.55 D²

+5.67 E²

ANOVA for Reduced Quadratic model

Response 4: Mn

Source	Sum of Squares	df	Mean Square	F-value	p-value	
Model	20737.88	12	1728.16	6.74	0.0002	significant
A-Concentration	1379.47	1	1379.47	5.38	0.0330	
B-Temperature	3697.83	1	3697.83	14.43	0.0014	
C-Time	455.45	1	455.45	1.78	0.2001	
D-L/S	616.54	1	616.54	2.41	0.1393	
E-H2O2 Con.	4263.51	1	4263.51	16.63	0.0008	
AB	1056.25	1	1056.25	4.12	0.0583	
AC	4160.25	1	4160.25	16.23	0.0009	
AE	992.25	1	992.25	3.87	0.0657	
BD	1369.00	1	1369.00	5.34	0.0336	
BE	784.00	1	784.00	3.06	0.0983	

DE	676.00	1	676.00	2.64	0.1228	
A²	1108.90	1	1108.90	4.33	0.0530	
Residual	4357.32	17	256.31			
Lack of Fit	3251.32	14	232.24	0.6299	0.7631	not significant
Pure Error	1106.00	3	368.67			
Cor Total	25095.20	29				

Fit Statistics

Std. Dev.	16.01	**R²**	0.8264
Mean	60.60	**Adjusted R²**	0.7038
C.V. %	26.42	**Predicted R²**	0.3687
		Adeq Precision	9.0113

Final Equation in Terms of Coded Factors

Mn   =

+66.71

+8.21 A

+13.70 B

+4.79 C

-5.49 D

+14.77 E

+8.13 AB

+16.13 AC

-7.87 AE

+9.25 BD

-7.00   BE

-6.50   DE

-9.62   A²

10.3 ANOVA tables and Statistics for HNO_3

ANOVA for Reduced Quadratic model

Response 1: Li (1)

Source	Sum of Squares	df	Mean Square	F-value	p-value	
Model	14278.36	13	1098.34	39.62	< 0.0001	significant
A-Concentration	756.93	1	756.93	27.31	< 0.0001	
B-Temperature	3190.82	1	3190.82	115.11	< 0.0001	
C-Time	523.04	1	523.04	18.87	0.0005	
D-L/S	1116.95	1	1116.95	40.29	< 0.0001	
E-H2O2 Con.	1638.94	1	1638.94	59.13	< 0.0001	
AB	180.33	1	180.33	6.51	0.0214	
BC	725.16	1	725.16	26.16	0.0001	
BE	494.55	1	494.55	17.84	0.0006	
DE	184.18	1	184.18	6.64	0.0202	
A²	1186.08	1	1186.08	42.79	< 0.0001	
B²	1490.53	1	1490.53	53.77	< 0.0001	
D²	260.70	1	260.70	9.41	0.0074	
E²	560.15	1	560.15	20.21	0.0004	
Residual	443.51	16	27.72			
Lack of Fit	441.33	14	31.52	28.87	0.0340	significant
Pure Error	2.18	2	1.09			

Cor Total   14721.87   29

Fit Statistics

Std. Dev.	5.26	**R²**	0.9699
Mean	75.66	**Adjusted R²**	0.9454
C.V. %	6.96	**Predicted R²**	0.8896
		Adeq Precision	22.5586

Final Equation in Terms of Actual Factors

Li   =

-112.21542

+80.19532   Concentration

+3.49641   Temperature

+0.572404   Time

+643.17168 L/S

+61.25497   H2O2 Con.

+0.315811   Concentration * Temperature

-0.008852   Temperature * Time

-0.519686   Temperature * H_2O_2 Con.

+253.20007 L/S * H_2O_2 Con.

-41.29558   Concentration²

-0.026095   Temperature²

-3896.65771 L/S²

-32.94187 H_2O_2 Con.²

ANOVA for Reduced Quadratic model

Response 2: Co

Source	Sum of Squares	df	Mean Square	F-value	p-value	
Model	19889.72	12	1657.48	18.24	< 0.0001	significant
B-Temperature	802.76	1	802.76	8.83	0.0085	
D-L/S	934.43	1	934.43	10.28	0.0052	
E-H2O2 Con.	7857.58	1	7857.58	86.46	< 0.0001	
AB	282.84	1	282.84	3.11	0.0957	
AC	291.11	1	291.11	3.20	0.0913	
AD	317.44	1	317.44	3.49	0.0790	
BC	438.32	1	438.32	4.82	0.0422	
BE	314.89	1	314.89	3.47	0.0801	
A^2	803.99	1	803.99	8.85	0.0085	
B^2	284.31	1	284.31	3.13	0.0949	
D^2	931.02	1	931.02	10.24	0.0052	
E^2	3716.62	1	3716.62	40.90	< 0.0001	
Residual	1544.91	17	90.88			
Lack of Fit	1455.62	15	97.04	2.17	0.3601	not significant
Pure Error	89.29	2	44.65			
Cor Total	21434.63	29				

Fit Statistics

Std. Dev. 9.53	**R²**	0.9279	
Mean 69.21	**Adjusted R²**	0.8770	
C.V. % 13.77	**Predicted R²**	0.7791	
	Adeq Precision	13.5823	

Final Equation in Terms of Coded Factors

Co   =

+100.72

+6.62   B

+7.33   D

+21.96 E

+4.59   AB

+4.66   AC

-5.66   AD

-5.40   BC

-4.86   BE

-8.49   A²

-5.77   B²

-8.16   D²

-21.84 E²

ANOVA for Reduced Quadratic model

Response 3: Ni

Source	Sum of Squares	df	Mean Square	F-value	p-value
Model	9712.99	10	971.30	8.19	< 0.0001 significant
B-Temperature	1158.74	1	1158.74	9.77	0.0056
D-L/S	886.33	1	886.33	7.47	0.0132
AD	1065.11	1	1065.11	8.98	0.0074
BC	362.53	1	362.53	3.06	0.0966
BD	1429.07	1	1429.07	12.05	0.0026
CD	398.12	1	398.12	3.36	0.0827

DE	278.36	1	278.36	2.35	0.1420	
A²	334.98	1	334.98	2.82	0.1092	
C²	1203.42	1	1203.42	10.15	0.0049	
D²	961.45	1	961.45	8.11	0.0103	
Residual	2253.80	19	118.62			
Lack of Fit	2106.89	17	123.93	1.69	0.4361	not significant
Pure Error	146.91	2	73.45			
Cor Total	11966.79	29				

Fit Statistics

Std. Dev.	10.89	**R²**	0.8117
Mean	67.34	**Adjusted R²**	0.7125
C.V. %	16.17	**Predicted R²**	0.5784
		Adeq Precision	11.7971

Final Equation in Terms of Coded Factors

Ni   =

+82.26

+8.36 B

+7.48 D

-8.85 AD

-5.36 BC

-11.35 BD

-6.07 CD

-4.72 DE

-5.52 A²

-11.18 C²

-8.26   D²

ANOVA for Reduced Quadratic model

Response 4: Mn

Source	Sum of Squares	df	Mean Square	F-value	p-value	
Model	12217.06	10	1221.71	6.57	0.0002	significant
B-Temperature	1536.67	1	1536.67	8.26	0.0097	
C-Time	959.85	1	959.85	5.16	0.0349	
D-L/S	3081.52	1	3081.52	16.57	0.0007	
E-H2O2 Con.	1457.00	1	1457.00	7.84	0.0114	
AB	498.18	1	498.18	2.68	0.1181	
AC	464.17	1	464.17	2.50	0.1306	
BC	307.86	1	307.86	1.66	0.2137	
B²	839.74	1	839.74	4.52	0.0469	
D²	2088.90	1	2088.90	11.23	0.0034	
E²	402.94	1	402.94	2.17	0.1574	
Residual	3533.12	19	185.95			
Lack of Fit	3481.00	17	204.76	7.86	0.1187	not significant
Pure Error	52.11	2	26.06			
Cor Total	15750.17	29				

Fit Statistics

Std. Dev.	13.64	**R²**	0.7757
Mean	72.98	**Adjusted R²**	0.6576
C.V. %	18.68	**Predicted R²**	0.4317
		Adeq Precision	10.2918

Final Equation in Terms of Coded Factors

Mn   =

+93.22

+9.11 B

+7.18 C

+13.54 D

+9.23 E

+5.74 AB

+5.54 AC

-4.51 BC

-9.72 B²

-12.24 D²

-6.86 E²

10.4 Environmental impacts of each component for different inorganic acids to leach 1 kg of Li